RSC Advances

PAPER

View Article Online
View Journal | View Issue

Cite this: *RSC Adv.*, 2025, **15**, 541

Remarkable utilization of quinazoline-based homosulfonamide for *in vitro* cytotoxic effects with triple kinase inhibition activities: cell cycle analysis and molecular docking profile †

Adel S. El-Azab, * Alaa A.-M. Abdel-Aziz, Ahmed H. Bakheit, Hamad M. Alkahtani, Ahmad J. Obaidullah, Mohamed M. Hefnawy and Ibrahim A. Al-Suwaidan

We tested newly synthesized compounds **1–13** on 59 cancer cell lines and found that acylhydrazones **5**, **6**, **7**, **9**, and **12** showed the best *in vitro* cytotoxic activity. They stopped the mean growth percentage (MG%) by an average of 23.5, 55.2, 89.4, 88.5, and 88.4%, respectively. Compound **5** was subjected to NCI tests at five-dose dilutions on 59 tumor cells. It is more effective in killing tumor cells than gefitinib (mean GI_{50}: 7.7 μM) and erlotinib (mean GI_{50}: 2.1 μM). Its mean GI_{50} value was 1.0 μM, and its LC_{50} value was over 100 μM, whereas gefitinib's was 95.6 μM and erlotinib's was 14.3 μM. Its TGI was 89.2 μM, while those drugs were 66.3 and 14.3 μM, respectively. We evaluated acylhydrazones **5**, **6**, **7**, **9**, and **12** for dose-dependent enzymatic inhibition of EGFR, HER2, and CDK9 kinases to study the mechanism of the *in vitro* cytotoxicity. With IC_{50} values of 84.4 and 51.5 nM, compounds **5** and **6** are the most potent EGFR inhibitor analogs, similar to Gefitinib (IC_{50} of 53.1 nM). Compounds **5**, **6**, and **12** blocked HER2 like Gefitinib did (IC_{50} = 38.8 nM); their IC_{50} values were 53.9, 44.1, and 110.6, respectively. Compounds **5**, **6**, and **7** had IC_{50} values of 146.9, 96.1, and 155.4 nM, which means they blocked CDK9 activity almost as well as Dinaciclib (IC_{50} 53.1 nM). Flow cytometers count the amount of DNA in T-47D and MOLT4 cells treated with compounds **5** and **6**. The IC_{50} value of compound **5** increases from 6.6% for the DMSO/T-47D control to 26.3% in the G2-M phase, while compound **6** goes from 61.4 for the DMSO/MOLT4 control to 89.0% in the G1 phase. The tested compounds cause early death, ranging from 0.4% and 0.6% (a DMSO control sample) to 9.3% and 19.2%, respectively. Derivatives **5** and **6** also increased late death from 0.1 to 14.8% and 12.6 to 0.3%, respectively, favoring the apoptotic route over the necrotic one for cell death to 50.5 μM. When tested for cell death against the standard WI-38 fibroblast cell line, imines **5** and **6** were less toxic than doxorubicin.

Received 5th October 2024
Accepted 26th December 2024

DOI: 10.1039/d4ra07174c

rsc.li/rsc-advances

1 Introduction

A failure of certain enzymes and proteins that control cell division and transformation causes cancer, characterized by abnormal cell growth.[1,2] Cancer is one of the most critical causes of death, with about 10 million deaths on average during the last few years.[3] The quinazoline nucleus is one of the primary heterocyclic compounds with cytotoxic activity.[4–7] Multikinase inhibitors with high selectivity and efficacy contain quinazoline moieties like erlotinib (**I**), afatinib (**II**), and gefitinib (**III**), which are effective chemotherapeutic agents (Fig. 1). Epidermal growth factor receptors (EGFRs) belong to the family of sizeable transmembrane growth factor receptors (PTKs), including homologous receptors such as HER1, HER2, HER3, and HER4.[8] Many malignancies, such as colon, breast, ovarian, and NSC lung cancers, are characterized by overexpression of EGFRs.[8] Designing a cytotoxic molecule that binds to the target enzyme's catalytic domain and treats different types of human cancers that compete with ATP, like an EGFR inhibitor, could be a primary method for a cytotoxic molecule.[8] Chemotherapy has been one of the best methods for treating cancer. Hence, synthesizing new cytotoxic molecules with potential bioactivity and a high therapeutic index is the main goal for many pharmaceutical and medicinal researchers. Compounds containing a quinazoline core, on the other hand, exhibit inhibitor activities, such as COX-2,[9–12] and carbonic anhydrase inhibitors,[13–17] as well as tyrosine kinase inhibitor activities, such as EGFRs, CDK-9,[18–27] anticonvulsant[28–31] cytotoxic activity,[32–39] and antimicrobial.[40–43] Schiff base derivatives, such as aldimines or

Department of Pharmaceutical Chemistry, College of Pharmacy, King Saud University, P.O. Box 2457, Riyadh 11451, Saudi Arabia. E-mail: adelazab@ksu.edu.sa

† Electronic supplementary information (ESI) available. See DOI: https://doi.org/10.1039/d4ra07174c

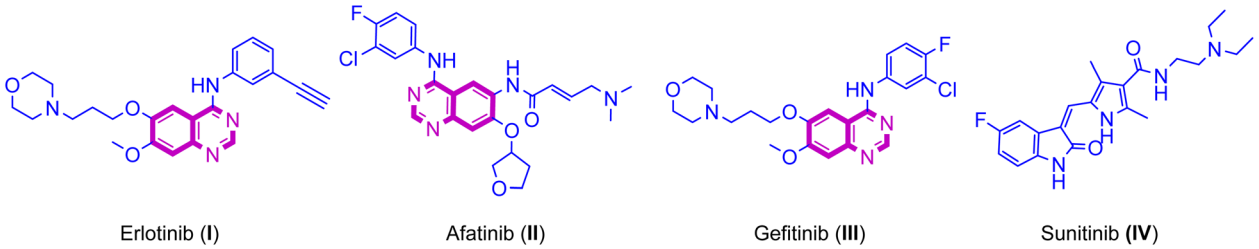

Fig. 1 The EGFR and HER2 inhibitors antitumor agent (I–IV).

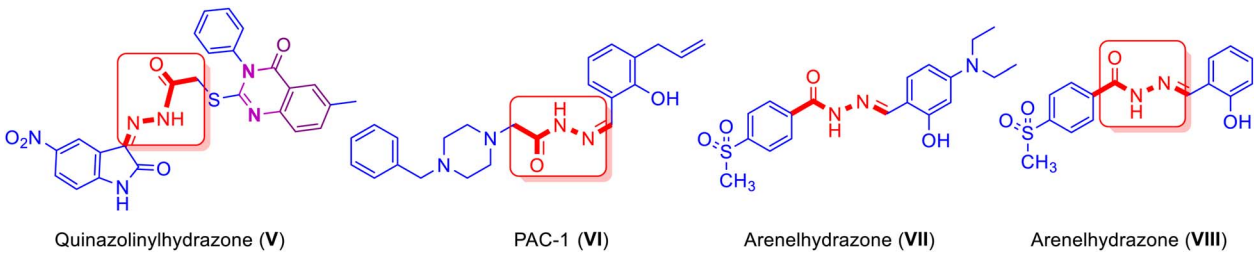

Fig. 2 The reported hydrazones with antitumor activities.

ketamine,[44,45] can bind to and block EGFRs by interacting with their ATP-binding site, showing cytotoxic activities.[45,46] Sulfonamides also showed many pharmacologic activities.[47–60] Fig. 2 also shows several hydrazones that kill cancer cells, such as quinazolinylhydrazone (**V**) and PAC-1 (**VI**); arylhydrazone (**VII** and **VIII**) showed cytotoxic activity higher than erlotinib, gefitinib, and sorafenib against several human cancer cells.[61–65] Some hydrazones stop cancer cells from growing by blocking EGFR, HER2, and COX-2 receptors.[61–65] Here, aldimines and ketimines (**4–13**) are formed (Fig. 3) by combining various aldehydes or ketones with 4-((4-oxo-2-thioxo-1,4-dihydroquinazolin-3(2*H*)-yl)methyl)benzenesulfonamide (**1**). We investigated the *in vitro* cytotoxic efficacy of target compounds *in vitro* in 59 human cancer cell lines, revealing the structure–activity relationship (SAR). We then used an enzymatic assay on effective cytotoxic acylhydrazones to determine EGFR, HER2,

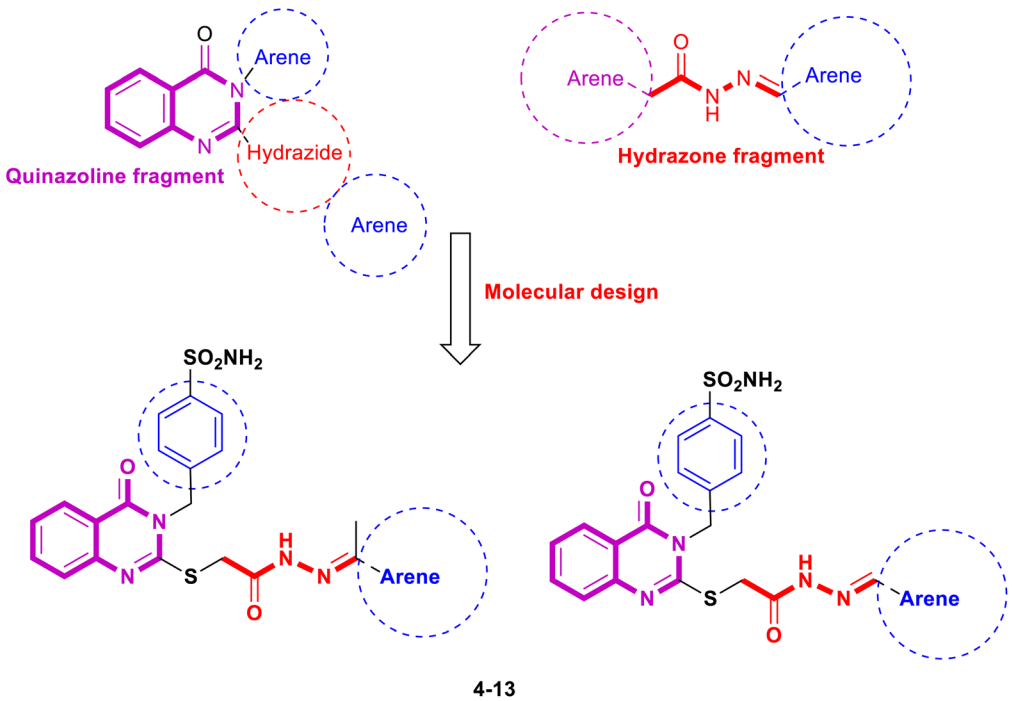

Fig. 3 The designed target quinazolinylhydrazone derivative (compounds **4–13**) are based on the chemical structures of compounds I–XI.

CDK9, and COX-2 inhibitions. We triggered apoptosis and examined cell cycles on the most active compounds to assess their *in vitro* cytotoxic potential. We performed molecular docking in the binding pockets of the EGFR, HER2, and CDK9 kinases to explore how the potential variants might line up.

2 Result and discussion

4-((4-Oxo-2-thioxo-1,4-dihydroquinazolin-3(2*H*)-yl)methyl)benzenesulfonamide (**1**) was obtained in excellent yield by the heating of 2-aminobenzoic acid with 4-isothiocyanatobenzenesulfonamide in ethanol (Scheme 1). Confirmation of the compound **1** structure was provided by the presence of the thioamide (NHCS) singlet peak at 13.15 ppm and doublet (NH_2) peak of the sulfonamide moiety at 7.34 ppm, together with the singlet methylene peak of the phenylmethansulfonamide moiety at 5.37 ppm in ^{1}H NMR. At the same time, ^{13}C NMR showed a thioketone (NHCS) at 175.89 ppm and benzylic methylene peaks at 49.11 ppm, respectively. The reaction of compound **1** with ethyl 2-bromoacetate in acetone and potassium carbonate was a crucial step in our research. This reaction led to the formation of the ethyl 2-((4-oxo-3-(4-sulfamoylbenzyl)-3,4-dihydroquinazolin-2-yl)thio)acetate (**2**). The singlet thiomethylencarbonyl peak (–

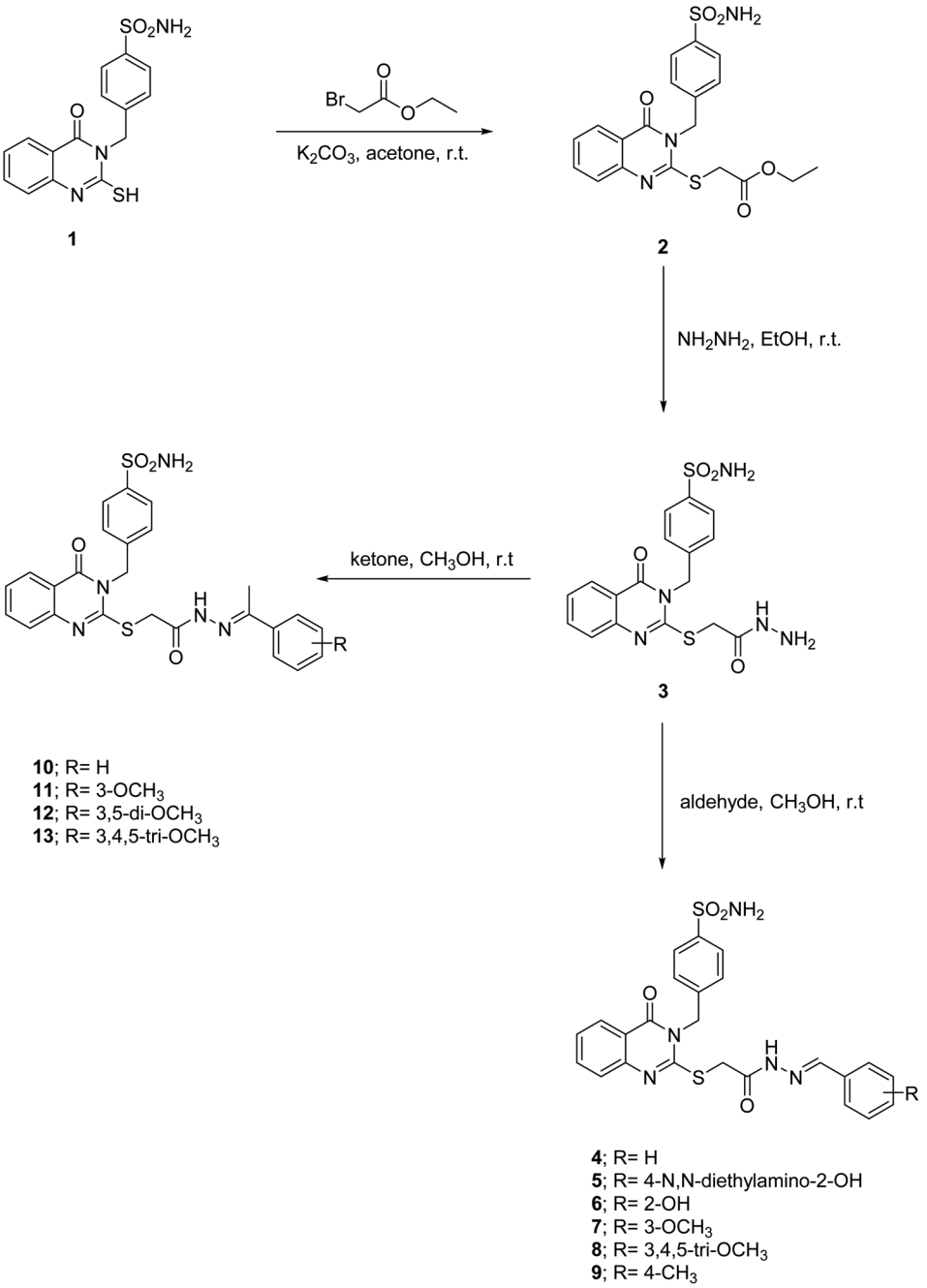

Scheme 1 Synthesis of ester **2**, acidhydrazide **3**, acylhydrazones **4**–**13** based on quinazolines incorporating benzylulfonamide.

Table 1 *In vitro* cytotoxic activity of 2-substituted-mercaptoquinazoline derivatives **1–13** presented as growth inhibition percentages (GI%) for 59 subpanel tumor cell lines[a]

Compound no.	PCE*	Cancer cell line assays (10.0 μM in one dose, GI %)	**MG%
1	4/59	Non-small cell Lung (HOP-92, 14%), C.N.S. (SNB-75, 23%), and Renal (CAKI-1, 11%; UO-31, 19%)	97.13
2	2/59	CNS (SNB-75, 15%), and Renal (UO-31, 16%)	100.32
3	0/59	—	104.42
4	9/59	Non-Small Cell Lung (EKVX, 14%; NCI–H522, 18%), CNS (SNB-75, 13%), Melanoma (UACC-62, 11%), Renal (CAKI-1, 16%; UO-31, 21%), Breast (MCF-7, 14%; MDA-MB-231/ATCC, 12%; HS-578T, 11%)	99.39
5	59/59	Leukemia (CCRF-CEM, 90%; HL-60(TB), 120%; K-562, 94%, MOLT-4, 89%; RPMI-8226, 83%; SR, 90%), Non-Small Cell Lung (A549/ATCC, 71%; EKVX, 65%; HOP-62, 79%; HOP-92, 42%; NCI-H226, 69%; NCI-H23, 61%; NCI-H322M, 67%; NCI-H460, 94%; NCI-H522, 126%), Colon (COLO-205, 102%; HCC-2998, 80%; HCT-116, 79%; HCT-15, 53%; HT-29, 68%; KM-12, 85%; SW-620, 79%), CNS (SF-268, 82%; SF-295, 80%; SF-539; 72%; SNB-19, 59%; SNB-75, 62%; U-251, 76%), Melanoma (LOX IMVI, 99%; MALME-3M, 69%; M14, 96%; MDA-MB-435, 87%; SK-MEL-2, 90%; SK-MEL-28, 67%; SK-MEL-5, 95%; UACC-257, 87%; UACC-62, 94%), Ovarian (IGROV1, 74%; IGROV-3, 85%; IGROV-4, 88%; IGROV-5, 45%; OVCAR-8, 80%; NCI/ADR-RES, 13%; SK-OV-3, 79%), Renal (786-0, 68%; ACHN, 67%; CAKI-1, 69%; RXF 393, 58%; SN-12C, 68%; TK-10, 85%; UO-31, 54%), Prostate (PC-3, 51%; DU-145, 62%), Breast (MCF-7, 87%; MDA-MB-231/ATCC, 75%; HS-578T, 37%; BT-549, 67%; T-47D, 94%; MDA-MB-468, 110%).	23.46
6	58/59	Leukemia (CCRF-CEM, 77%; HL-60(TB), 60%; K-562, 64%, MOLT-4, 80%; RPMI-8226, 51%; SR, 76%), Non-Small Cell Lung (A549/ATCC, 31%; EKVX, 40%; HOP-62, 65%; HOP-92, 46%; NCI-H226, 43%; NCI-H23, 37%; NCI-H322M, 53%; NCI-H460, 51%; NCI-H522, 101%), Colon (COLO-205, 71%; HCC-2998, 50%; HCT-116, 58%; HCT-15, 25%; HT-29, 14%; KM-12, 61%; SW-620, 40%), CNS (SF-268, 62%; SF-295, 35%; SF-539; 46%; SNB-19, 45%; SNB-75, 15%; U-251, 57%), Melanoma (LOX IMVI, 84%; MALME-3M, 41%; M14, 58%; MDA-MB-435, 29%; SK-MEL-2, 64%; SK-MEL-28, 43%; SK-MEL-5, 42%; UACC-257, 30%; UACC-62, 62%), Ovarian (IGROV1, 38%; IGROV-3, 87%; IGROV-4, 60%; IGROV-5, 32%; OVCAR-8, 56%; SK-OV-3, 37%), Renal (786-0, 29%; ACHN, 28%; CAKI-1, 46%; RXF 393, 28%; SN-12C, 44%; TK-10, 47%; UO-31, 39%), Prostate (PC-3, 33%; DU-145, 28%), Breast (MCF-7, 50%; MDA-MB-231/ATCC, 70%; HS-578T, 29%; BT-549, 44%; T-47D, 67%; MDA-MB-468, 48%).	55.22
7	29/59	Leukemia (CCRF-CEM, 46%; HL-60(TB), 16%; K-562, 40%, MOLT-4, 36%; RPMI-8226, 56%; SR, 17%), Non-Small Cell Lung (A549/ATCC, 14%; HOP-62, 14%; NCI-H23, 16%; NCI-H522, 30%), Colon (HCT-15, 26%; KM-12, 11%), CNS (SF-268, 15%; SF-295, 23%; SNB-75, 18%), Melanoma (LOX IMVI, 21%; SK-MEL-2, 19%; 67%; SK-MEL-5, 32%; UACC-62, 33%), Ovarian (IGROV1, 15%; IGROV-4, 10%; OVCAR-8, 23%), Renal (CAKI-1, 16%; SN-12C, 11%; UO-31, 29%), Prostate (PC-3, 18%), Breast (MCF-7, 17%; MDA-MB-231/ATCC, 13%; T-47D, 36%).	89.35
8	15/59	Leukemia (RPMI-8226, 13%), Non-Small Cell Lung (EKVX, 15%; NCI-H226, 11%; NCI-H322M, 15%; NCI-H522, 48%), CNS (SF-268, 15%; SF-539, 12%;), Renal (CAKI-1, 14%; RXF 393, 10%; SN-12C, 10%; UO-31, 25%), Breast (MCF-7, 11%; MDA-MB-231/ATCC, 15%; HS-578T, 15%; MDA-MB-468, 19%).	96.77
9	28/59	Leukemia (CCRF-CEM, 13%; K-562, 37%, MOLT-4, 14%; SR, 51%), Non-Small Cell Lung (A549/ATCC, 15%; EKVX, 10%; NCI-H226, 16%; NCI-H522, 58%), Colon (HCT-15, 11%; HT-29, 14%; KM-12, 14%), CNS (SF-268, 22%; SNB -19, 11%; SNB-75, 29%), Melanoma (LOX IMVI, 18%; MDA-MB-435, 54%; SK-MEL-5, 26%; UACC-62, 22%), Ovarian (OVCAR-3, 21%), Renal (CAKI-1, 36%; RXF 393, 14%; UO-31, 20%), Prostate (PC-3, 11%), Breast (MCF-7, 41%; MDA-MB-231/ATCC, 11%; HS-578T, 12%; T-47D, 19%; MDA-MB-468, 19%).	88.50
10	6/59	Non-small cell Lung (EKVX, 10%; NCI-H322M, 14%), CNS (SF-268, 14%; U-251, 15%), and Renal (CAKI-1, 16%; UO-31, 20%).	100.92
11	17/59	NSC Lung (NCI-H522, 52%), Colon (HCT-116, 20%), C.N.S. (SF-268, 25%; SF-539; 28%; SNB-19, 15%; SNB-75, 22%; U-251, 20%), Melanoma (SK-MEL-5, 10%), Ovarian (OVCAR-5, 12%), Renal	94.54

Table 1 (*Contd.*)

Compound no.	PCE*	Cancer cell line assays (10.0 μM in one dose, GI %)	**MG%
		(CAKI-1, 21%; RXF 393, 16%; UO-31, 21%), Breast (M.C.F.-7, 10%; MDA-MB-231/ATCC, 25%; HS-578T, 19%; T-47D, 11%; MDA-MB-468, 19%).	
12	25/59	Leukemia (SR, 28%), N.S.C. Lung (NCI-H23, 17%; NCI-H522, 62%), Colon (HCT-116, 17%; KM-12, 30%), CNS (SF-268, 64%; SF-539; 64%; SNB-19, 49%; SNB-75, 39%; U-251, 26%), Melanoma (LOX IMVI, 20%; MALME-3M, 30%; M14, 11%; MDA-MB-435, 30%; SK-MEL-5, 32%; UACC-62, 17%), Ovarian (OVCAR-5, 14%), Renal (786-0, 15%; CAKI-1, 16%; RXF 393, 30%), Breast (MDA-MB-231/ATCC, 28%; HS-578T, 11%; BT-549, 57%; T-47D, 62%; MDA-MB-468, 27%).	88.40
13	8/59	Leukemia (S.R., 12%), C.N.S. (SNB-75, 13%), Renal (CAKI-1, 15%; UO-31, 24%), Breast (M.C.F.-7, 11%; MDA-MB-231/ATCC, 11%; T-47D, 15%; MDA-MB-468, 16%)	97.44
Imatinib	20/59	Leukemia (MOLT-4, 18%; PRMI-8226, 12.6%; SR, 14.6%), N.S.C. Lung (EKVX, 15.7%; NCI-H226, 10.6%; NCI-H23, 17.1%), Colon (HCT-116, 18.6%; HCT-15, 11.5%; HT-29, 47.1%), CNS (SF-295, 15.1%; SF-539, 24.5%; U251, 10.6%), Melanoma (LOX IMVI, 11.6%; SK-MEL-5, 22.3%), Renal (A-498, 13.7%), Prostate (PC-3, 10.6%; DU-145, 14.4%), Breast (MDA-MB-231/ATCC, 11.2%; T-47D, 18.6%; MDA-MB-468, 29.1%)	92.62%

[a] *Most sensitive cell lines PCE: positive cytotoxic effect is defined as the ratio between the number of cell lines with percentage growth inhibition of >10% and the total number of cell lines **: mean growth percent.

SCH_2CO–) at 4.11 ppm in ^{1}H NMR, the quartet and triplet peaks of the ethoxide moiety (OCH_2CH_3) at 4.14 and 1.21 ppm, respectively, and fading of the thioamide (NH) singlet peak at 13.15 ppm confirming ester **2**. ^{13}C NMR of the ester **2** reveals the presence of thiomethylene peak (–SCH_2) at 47.13 ppm and carbonyl (C=O) peaks at 168.58 ppm of the thiomethylenecarbonyl group (–SCH_2C=O), the ethoxide peaks (OCH_2CH_3) at 61.58 and 14.61 ppm, respectively, and the disappearance of the thione group (C=S) at 175.89 ppm, which supported the structure conformation. 4-((2-((2-Hydrazineyl-2-oxoethyl)thio)-4-oxoquinazolin-3(4*H*)-yl)methyl)benzenesulfonamide (**3**) are obtained by stirring ester derivative **2** with hydrazine hydrate in ethanol. The acid hydrazide **3** was confirmed by the disappearance of ethoxide peaks (OCH_2CH_3) at (4.14 and 1.21 ppm) and (61.58 and 14.61 ppm) in ^{1}H NMR and ^{13}C NMR spectra, respectively. Additionally, it strongly supported the structure confirmation presence of the amidic proton (CONH–) peak at 9.40 ppm and (NH_2) singlet peaks at 4.38 and 4.32 ppm due to an acid hydrazide moiety ($CONHNH_2$) in ^{1}H NMR and the carbonyl peak of an amide group (CONH) at 156.62 ppm in ^{13}C NMR. The aldimines **4–9** and ketimines **10–13** were obtained by the heating of 4-((2-((2-hydrazineyl-2-oxoethyl)thio)-4-oxoquinazolin-3(4*H*)-yl)methyl)benzenesulfonamide (**3**) in ethanol with various aldehydes and ketones. The formation of these imines **4–13** was confirmed by the disappearance of the singlet peaks of the amino group (NH_2) at 4.38 and 4.32 ppm in the ^{1}H NMR spectrum, which is attributed to the acid hydrazide moiety ($CONHNH_2$). Furthermore, the presence of the *E* and *Z* isomer peaks at 11.86–11.76 and 10.85–11.36 ppm of the imide group (CONH–), together with the olefinic protons of the imine group (CONH–N=*C*–*H*–) at 8.25–8.13 and 8.16–8.00 ppm in ^{1}H NMR, strongly supported the confirmation of aldimines **4–9**. Ketimines **10–13** were characterized by *E* and *Z* isomeric peaks at 10.97–10.93 and 10.80–10.77 ppm of the imide group (CONH–) in ^{1}H NMR, and the methyl peaks of the ethylidenehydrazineyl group (CONH–N=*C*–CH_3) at 2.34–2.30 and 2.30–2.27 ppm and 15.0–14.71 and 14.36–14.15 ppm in ^{1}H NMR and ^{13}C NMR respectively as isomeric mixtures.

2.1 Biological evaluation

2.1.1 ***In vitro*** **cytotoxic activity.** The NCI, Bethesda, MD, USA, assessed thirteen compounds **1–13** for their *in vitro* cytotoxic activity against the imatinib reference drug. They determined the growth inhibition percentage (GI%) against 59 cancer cell lines from various human tissues at a single treatment concentration of 10 μM (Table 1). The chemo-cytotoxicity of compounds **1–13** ranged from moderate to potent activity at a dose of 10 μM, with a mean growth rate (MG) of 104.4–23.5% compared to imatinib and the number of cell lines with growth inhibition > 10% (PCE) ranging from 6/59 to 59/59 (Table 1). Compounds **5**, **6**, **7**, **9**, and **12** had the highest PCE at 59/59, 58/59, 29/59, 28/59, and 25/59, respectively, with MG values of 23.5, 55.2, 89.4, 88.5, and 88.4%. Compounds **8** and **11** had PCEs of 15/59 and 17/59, respectively (MG = 96.8 and 94.5%), compared to imatinib PCE of 20/55 and MG value of 92.6%. Compounds **1–4** and **10** have the lowest PCE (0-9/59; MG = 104.42–97.1%). Derivatives **1–13** (Table 1) were evaluated against 59 cancer cells. Schiff bases **1**, **2**, **4**, **5**, **6**, **7**, **8**, **9**, **10**, **11**, **12**, and **13** showed GI values greater than 10–>100% against most cancer cell lines, whereas imatinib had GI values ranging from 10 to 47. Quinazolines **5**, **6**, **7**, **9**, and **12** exhibited substantial *in vitro* cytotoxic activity against leukemia (GI% = 13–120), NSCLC (GI% = 10–126), colon cancer (GI% = 11–80), CNS cancer (GI% = 11–82), melanoma (GI% = 11–99), ovarian cancer (GI% = 11–88), renal cancer (GI% = 11–87), prostate cancer (GI% = 11–62), and breast cancer (GI% = 11–110). In leukemia (GI% = 13–18), NSCLC (GI% = 11–17), colon cancer (GI% = 12–47), CNS cancer (GI% = 11–25), melanoma (GI% = 12–22), ovarian cancer (GI% < 10), renal cancer (GI% < 10–14), prostate cancer (GI% = 11–14), and breast cancer (GI% = 11–29), imatinib exhibited moderate antitumor activity.

Table 2 Median growth-inhibitory (GI_{50}, μM), total growth-inhibitory (TGI, μM), and median lethal (LC_{50}, μM) concentrations of compound **5** and reference drugs erlotinib (718 781) and gefitinib (759 856) on *in vitro* subpanel tumor cell lines μm[a]

		Subpanel tumor cell lines									
Compound	Activity	Leukemia	NSC lung cancer	Colon cancer	CNS cancer	Melanoma	Ovarian cancer	Renal cancer	Prostate cancer	Breast cancer	MG_MID[a]
5	GI_{50}	0.384	1.059	1.557	1.494	1.501	15.11	1.917	0.886	1.23	1.096
	TGI	68.371	c	c	c	59.09	c	91.54	c	84.17	89.24
	LC_{50}	c	c	c	c	c	c	c	c	c	c
Erlotinib	GI_{50}	27.85	13.11	51.68	16.99	23.74	5.52	2.46	20.90	24.72	7.68
	TGI	96.57	73.76	c	82.11	77.89	74.41	42.59	c	70.53	66.3
	LC_{50}	c	97.71	c	c	93.31	97.06	89.15	c	96.43	95.6
Gefitinib	GI50	2.56	2.05	5.23	5.64	3.68	3.05	1.41	3.29	4.67	2.10
	TGI	12.07	13.86	18.47	19.62	12.49	33.29	12.50	31.62	18.62	14.3
	LC_{50}	93.85	94.68	51.74	50.56	36.40	83.58	52.82	89.72	52.47	51.9

[a] [a]Full panel mean-graph midpoint (μM); [c] Compounds showed values > 100 μM; mean 50% cell growth inhibition (GI_{50}); total cell growth inhibition (TGI); median lethal concentration (LC_{50}); Mean GI_{50} graph midpoints (GI_{50} MG_MID).

2.1.2 Structure–activity relationship. Structure correlation analysis revealed that quinazolinthione **1**, ester **2**, and acid-hydrazide **3** had little tumor-killing efficacy (PCE = 4/59, 2/59, and 0/59, respectively). The conversion of acid-hydrazide **3** into hydrazones **4–9** resulted in different levels of *in vitro* cytotoxic activity, each higher than hydrazide 3 (PCE = 9/59–59/59). This group of hydrazones, including a 2-hydroxyphenyl moiety, like 5 and 6 (PCE = 59/59 and 58/59), was much better at killing tumor cells than compound with an unsubstituted phenyl **4** and methoxyphenyl derivative, including **7** and **8**, as well as the 3-tolyl derivative **9** (PCE = 9/59, 29/59, 15/59, and 28/59, respectively). Adding three methoxy groups to the phenyl ring, as in compound **8**, made it more effective against tumor cells (PCE = 15/59) than parent phenyl **4** (PCE = 9/59); however, it wasn't as effective as methoxyphenyl **7**, which had a PCE of 29/59. The conversion of acid-hydrazide **3** into ethylidene hydrazones **10–13** resulted in varying levels of *in vitro* cytotoxic activity higher than parent hydrazide **3** (PCE = 6/59–25/59).

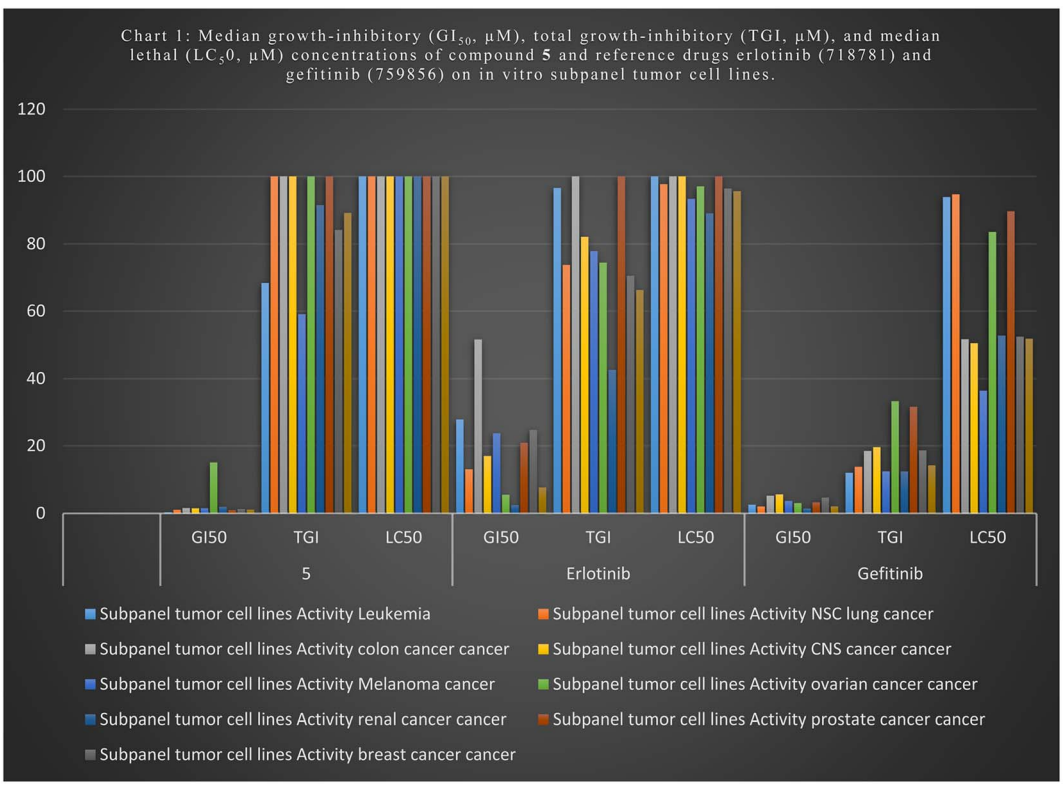

Chart 1 Median growth-inhibitory (GI_{50}, μM), total growth-inhibitory (TGI, μM), and median lethal (LC_{50}, μM) concentrations of compound **5** and reference drugs erlotinib (718 781) and gefitinib (759 856) on *in vitro* subpanel tumor cell lines.

Table 3 The GI_{50} values (μM) of compound **5** on *in vitro* subpanel tumor cell lines, compared to erlotinib and gefitinib[a]

Subpanel tumor cell lines	GI_{50} (μM)		
	5	Erlotinib	Gefitinib
Leukemia			
CCRF-CEM	0.196	15.84	5.01
HL-60(TB(K-562))	0.412	5.01	5.01
	0.592	15.48	2.51
MOLT-4	0.372	5.01	3.98
RPMI-8226	0.521	5.01	1.58
SR	0.212	6.30	3.16
Non-small cell lung cancer			
A549/ATCC	1.57	7.94	7.94
EKVX	0.650	0.005	0.005
HOP-62	0.961	12.58	10.00
HOP-92	nt	6.30	7.94
NCI-H226	0.894	6.30	15.84
NCI-H23	1.96	19.95	15.84
NCI-H322M	0.575	0.05	0.08
NCI-H460	0.424	5.01	6.30
NCI-H522	2.40	1.00	6.30
Colon cancer			
COLO 205	1.51	31.62	6.30
HCC-2998	0.882	79.34	10.00
HCT-116	0.363	5.01	7.94
HCT-15	3.62	3.16	5.01
HT29	3.01	50.11	3.98
KM12	0.569	63.09	7.94
SW-620	0.949	5.01	7.94
CNS cancer			
SF-268	0.766	19.95	7.94
SF-295	1.47	15.84	1.99
SF-539	1.26	12.58	10.00
SNB-19	2.10	3.98	12.58
SNB-75	2.86	12.58	6.30
U251	0.510	19.95	10.00
Melanoma			
LOX IMVI	0.387	5.01	7.94
MALME-3M	1.09	5.01	3.16
M14	0.452	6.30	5.01
MDA-MB-435	2.07	15.84	3.16
SK-MEL-2	2.41	12.58	12.58
SK-MEL-28	1.62	31.62	0.31
SK-MEL-5	1.57	15.84	3.98
UACC-257	3.03	100	6.30
UACC-62	0.886	1.25	5.01
Ovarian cancer			
IGROV1	0.785	0.25	0.20
OVCAR-3	0.287	3.16	5.01
OVCAR-4	0.311	19.95	7.94
OVCAR-5	2.09	19.95	10.00
OVCAR-8	0.932	7.94	10.00
NCI/ADR-RES	c	6.30	12.58
SK-OV-3	1.32	0.39	0.63
Renal cancer			
786-0	1.84	5.01	7.94
A498	nt	1.58	0.40
ACHN	1.58	0.15	0.20
CAKI-1	1.02	0.10	0.16
RXF 393	2.50	6.30	5.01
SN12C	1.93	6.3	6.30
TK-10	1.66	0.10	0.10
UO-31	2.89	1.99	1.25
Prostate cancer			
PC-3	0.829	50.11	0.79
DU-145	0.944	1.58	2.51
Breast cancer			
MCF7	0.457	100	10.00
MDA-MB-231/ATCC	0.643	1.99	12.58
HS 578T	2.11	6.30	10.00
BT-549	2.68	39.81	7.94
T-47D	0.925	3.16	6.30
MDA-MB-468	0.524	0.20	0.01

[a] nt = not tested; [c] compounds showed values > 100 μM.

Among ethylidene hydrazones, those with a methoxyphenyl group, like **11** and **12** (PCE = 17/59 and 25/59), were much better at killing tumors than those with an unsubstituted phenyl **10** (PCE = 6/59). The introduction of more than two methoxy groups to the phenyl ring, as in compound **13**, slightly increased its effectiveness against tumors (PCE = 8/59) compared to unsubstituted phenyl **10** (PCE = 6/59); however, it was not as potent as methoxyphenyl **11** and **12**, which had PCEs of 17/59 and 25/59, respectively. Hydrazones **4**, **5**, and **8** kill tumor cells more effectively (PCE = 9/59, 29/59, and 15/59, respectively) than the comparable ethylidene hydrazones **10**, **11**, and **13** (PCE = 6/59, 17/59, and 8/59, respectively).

2.1.3 GI_{50}, TGI, and LC_{50} of compound 5. Compound **5** is the most effective *in vitro* cytotoxic agent among the newly synthesized compounds, inhibiting the mean growth percentage (MG%) by an average of 23.5% (Table 1). NCI evaluated this compound on 59 tumor cells at five dosage dilutions.[62,63] For each cell, NCI assessed the mean 50% cell growth inhibition (GI_{50}), the total cell growth inhibition (TGI), and the median lethal concentration (LC_{50}) (Table 2 & Chart 1). With a mean (GI_{50} MG_MID) value of 1.096 μM, compound **5** is more effective at killing cells than erlotinib and gefitinib, which have (GI_{50} MG_MID) values of 7.7 and 2.1 μM, respectively. Additionally, compound **5** had a median lethal dose (LC_{50}) of more than 100 μM, which was higher than both gefitinib (95.6 μM) and erlotinib (14.3 μM). It also had a total cell growth inhibition (TGI) of 89.2 μM compared to those drugs (66.3 and 14.3 μM), respectively. Compound **5** had a GI_{50} value of 0.4 μM, which was higher cytotoxicity than erlotinib and gefitinib (27.9 and 2.6 μM) against leukemia, non-small cell lung cancer (1.1, 13.1, and 2.1 μM), colon cancer (1.6, 51.7, and 5.2 μM), CNS cancer (1.5, 17.0, and 5.6 μM), melanoma cancer (1.5, 23.7, and 3.7 μM), ovarian cancer (15.1, 20.9, and 3.3 μM), renal cancer (1.9, 2.5, and 1.4

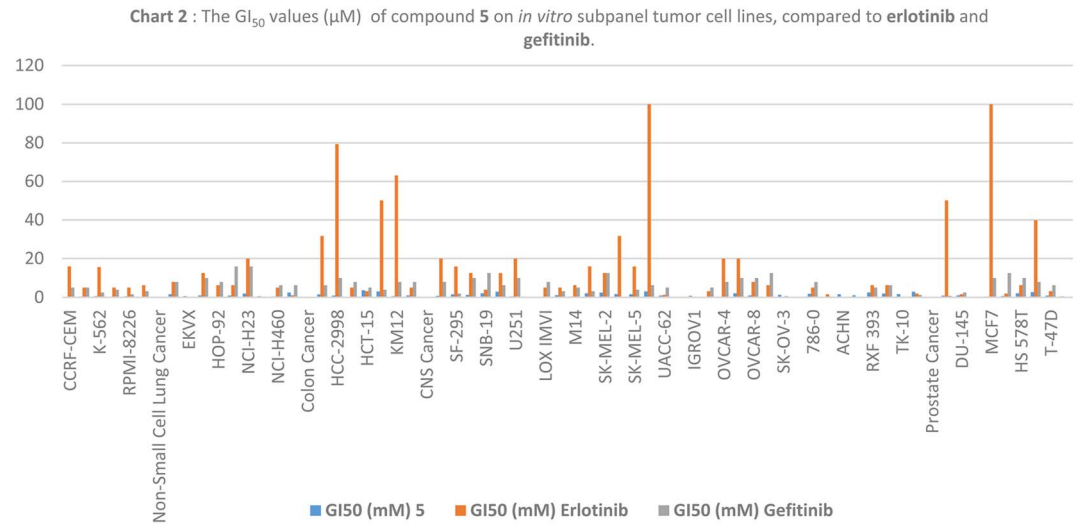

Chart 2 The GI_{50} values (μM) of compound **5** on *in vitro* subpanel tumor cell lines, compared to erlotinib and gefitinib.

μM), prostate cancer (0.9, 20.9, and 3.3 μM), and breast cancer (1.2, 24.7, and 4.7 μM) (Table 2 & Chart 1). In general, compound **5** could kill tumor cells with GI_{50} values (μM) that were about the same as or higher than erlotinib and gefitinib against most cell lines (Table 3 & Chart 2).

2.1.4 EGFR, HER2 and CDK9 kinase enzyme inhibition assay. We selected candidates **5**, **6**, **7**, **9**, and **12** because they had the highest *in vitro* cytotoxic activity against the tested cell lines. We conducted dose-related enzymatic inhibition against EGFR, HER2, and CDK9 kinases at different concentrations to determine their IC_{50} values in the nanomolar range. Table 4 demonstrates that compounds **5** and **6** have intense EGFR inhibitory action, with IC_{50} values in the nanomolar range. The

Table 6 Compounds **5** and **6** change the stained positive for annexin V-FITC of T-47D and MOLT4 cells at different IC_{50} concentration percentages values

	Apoptosis			
Compound no.	Total	Early	Late	Necrosis
5/T-47D	31.07	9.28	14.75	7.04
DMSO/T-47D	2.37	0.37	0.14	1.86
6/MOLT4	35.06	19.22	12.61	3.23
DMSO/MOLT4	1.71	0.55	0.31	0.85

Table 4 *In vitro* inhibitory effects of the quinazolines **5**, **6**, **7**, **9**, and **12** against COX-2, EGFR, HER2, and CDK9: the cytotoxicity of standard cell line (WI-38) for compounds **5** and **6**

	IC_{50}[a] nM				IC_{50}[a] (μM)
Compound no.	COX-2 inhibition	EGFR inhibition	HER2 inhibition	CDK9 inhibition	WI138
5	3.32 ± 0.06 (μM)	84.39 ± 2.07	53.91 ± 1.32	146.9 ± 3.60	45.326 ± 2.66
6	4.47 ± 0.09 (μM)	51.52 ± 1.26	44.13 ± 1.08	96.07 ± 2.35	27.772 ± 1.63
7	50.48 ± 1.06 (μM)	594.45 ± 14.5	387.01 ± 9.50	155.4 ± 3.81	—
9	15.41 ± 0.32 (μM)	377.53 ± 9.26	228.53 ± 5.61	316.40 ± 7.76	—
12	21.27 ± 0.44 (μM)	492.27 ± 12.1	110.64 ± 2.71	319.8 ± 7.85	—
Celecoxib	0.15 ± 0.003 (μM)	—	—	—	—
Gefitinib		53.12 ± 1.30	38.81 ± 0.95		—
Dinaciclib	—	—	—	53.12 ± 1.30	
Doxorubicin	—	—	—	—	9.57 ± 0.59

Table 5 Compounds **5** and **6** affect the cell cycle of T-47D and MOLT4 cells at their IC_{50} concentration levels compared to their DMSO control

Compound no.	%G0-G1	%S	%G2-M	Comment
Five/T-47D	46.31	27.42	26.27	Cell growth arrest at the G2/M phase
DMSO/T-47D	61.11	32.29	6.6	—
6/MOLT4	89.04	9.56	1.40	Cell growth arrest at the G1 phase
DMSO/MOLT4	61.37	22.54	16.09	—

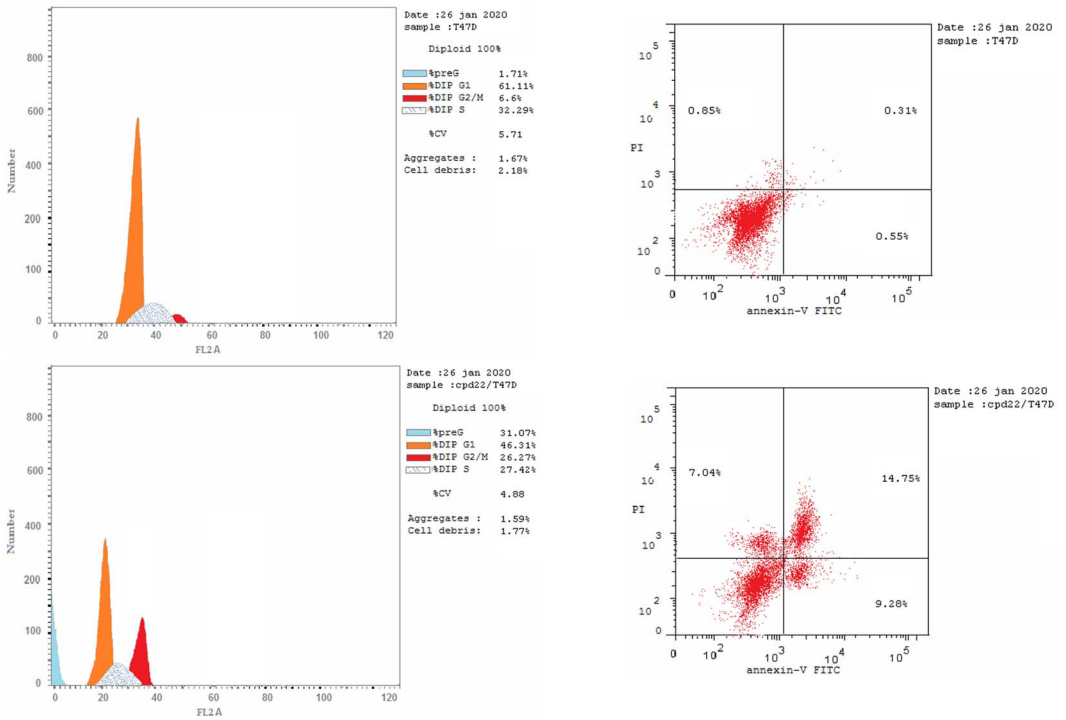

Fig. 4 Effect of DMSO (upper right panel) and **5** (lower right panel) on the percentage of annexin V-FITC-positive staining in MCF-7 cell. Cell cycle analysis of T47D cells treated with DMSO (upper left panel) and cell cycle analysis of T47D cells treated with compound 5 (lower left panel).

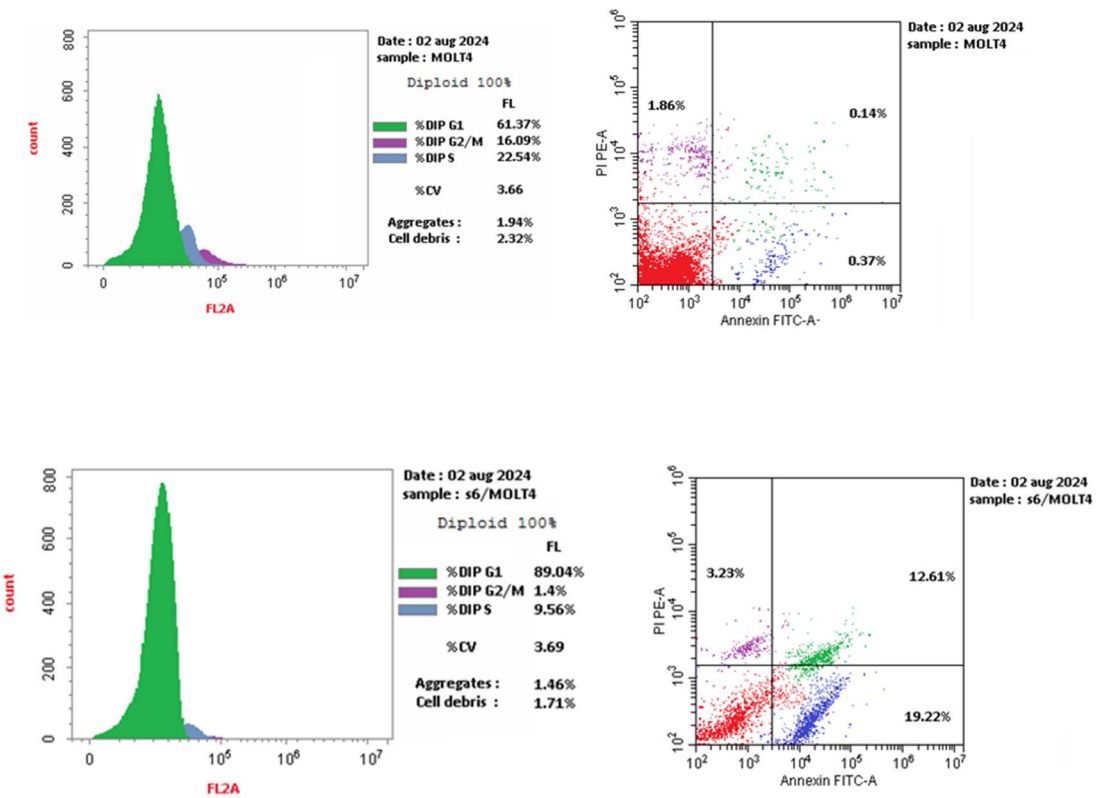

Fig. 5 Effect of DMSO (upper right panel) and **6** (lower right panel) on the percentage of annexin V-FITC-positive staining in MCF-7 cells. Cell cycle analysis of MOLT4 cells treated with DMSO (upper left panel) and MOLT4 cells treated with compound **6** (lower left panel).

Table 7 Compound **5** and Compound **6** hydrogen bond interactions with HER2, EGFR, and CDK9

Compound	Ligand	Receptor	Interaction	Distance	Binding affinities (kcal mol^{-1})
EGFR (PDB: 1XKK)					
5	C 15	OD2 ASP 855 (A)	H-donor	3.42	−8.513
	O 40	O SER 720 (A)	H-donor	3.01	
	O 26	N MET 793 (A)	H-acceptor	3.54	
	O 36	HA ASP 855 (A)	H-acceptor	3.33	
6	N 1	O LEU 788 (A)	H-donor	3.22	−8.109
	O 20	N MET 793 (A)	H-acceptor	3.67	
HER2 (PDB: 7PCD)					
5	O 38	O PHE 864 (A)	H-acceptor	3.83	−9.159
	N 21	HZ1 LYS 753 (A)	H-acceptor	3.84	
	O 14	OG1 THR 862 (A)	H-acceptor	3.35	
	O 26	N MET 801 (A)	H-acceptor	3.38	
	N 38	O LEU 796 (A)	H-donor	3.1	
6	O 20	N MET 801 (A)	H-acceptor	3.23	−7.854
	O 24	NZ LYS 753 (A)	H-acceptor	3.56	
	N 27	O LYS 860 (A)	H-acceptor	3.51	
	O 35	N ARG 784 (A)	H-acceptor	4.09	
CDK9 (PDB: 3BLR)					
5	O 26	N CYS 106 (A)	H-acceptor	3.47	−7.425
	N 38	OD1 ASP 109 (A)	H-donor	2.96	
6	N 1	OD2 ASP 109 (A)	H-donor	2.92	−7.656
	O 20	N CYS 106 (A)	H-acceptor	3.12	
	O 33	N LYS 151 (A)	H-acceptor	4.09	

most potent analogs, **5** and **6**, had IC_{50} values of 84.4 and 51.5 nM, which showed that they blocked EGFR similarly or much more effectively than the standard Gefitinib (IC_{50} of 53.1 nM). Compounds **7**, **9**, and **12** exhibited modest efficacy against EGFR with IC_{50} values of (377.5–594.5 nM). Also, compounds **5**, **6**, and **12** were relatively similar at inhibiting HER2 than Gefitinib (IC_{50} 38.8 nM), with IC_{50} values of 53.9, 44.1, and 110.6, respectively. Compounds **7** and **9** have less action than Gefitinib, with IC_{50} values of 387.0 and 228.5 nM, respectively. Also, compounds **5**, **6**, and **7** had IC_{50} values of 146.9, 96.1, and 155.4 nM, which were almost as strong at stopping CDK9 activity as Dinaciclib (IC_{50} 53.1 nM). Compounds **9** and **12** are less active than Dinaciclib, having IC_{50} values of 316.4 and 319.8 nM, respectively. Compared to Celecoxib, which has an IC_{50} value of 0.15 μM, Schiff bases **5**, **6**, **7**, **9**, and **12** did not exhibit any inhibition activity against COX-2, with IC_{50} values ranging from 3.3 to 50.5 μM (Table 4).

2.2 Structure–activity relationship

Based on the data, we can conclude that the Schiff base series with a 2-hydroxyphenyl group on the acylhydrazone moiety is the most potent kinase inhibitor against EGFR (IC_{50}; 84.4 and 51.5 nM), HER2 (IC_{50}; 53.9 and 44.1 nM), and CDK9 (IC_{50}; 146.9 and 96.1 nM), as compounds **5** and **6**, respectively. Schiff base with a 3-methoxyphenyl group on the acylhydrazone moiety, such as compound **7**, showed a potent CDK9 kinase inhibitor with an IC_{50} value of 155.4 nM, while compound **12** with the (3,5-dimethoxyphenyl)ethylidene)hydrazineyl) moiety showed vigorous HER2 kinase inhibitor activity with an IC_{50} value of 110.6 nM.

2.3 *In vitro* cytotoxicity against WI-38 fibroblast cell line

The most active kinase inhibitors, acylhydrazones **5** and **6**, were less toxic than doxorubicin when measured for their safety margin cytotoxicity against the standard WI-38 fibroblast cell line with IC50 values of 45.3 and 27.8 μM, respectively, compared to 9.6 μM for doxorubicin Table 4.

2.4 Cell cycle arrest analysis and apoptosis detection

We are studying cell cycle arrest and apoptosis in T-47D and MOLT4 cells to determine the role of our promising derivatives **5** and **6** in the cell cycle (Tables 5 and 6). Flow cytometry assays quantify the DNA content. After being treated with compounds **5** and **6**, the number of cells in the S phase dropped from 32.3 percent for DMSO-control cells to 20.9 percent for T-47D cells and 22.5 percent for MOLT4 cells. Also, compound **5** stopped the cells in the G2/M stage, raising the percentage of T-47D cells in the G2-M phase from 6.6% in the control cell to 26.3%. Acylhydrazone **6** stopped the cells in the G1 stage, lowering the percentage of MOLT4 cells in the G0-G1 phase from 89.0% in the control cell to 61.4%. Acylhydrazone **6** lowered the percentage of MOLT4 cells in the G0-G1 phase from 89.0% in the control cell to 61.4% at the G1 stage. Furthermore, compounds **5** and **6** boosted early apoptosis from 0.4 and 0.6 (DMSO control sample) to 9.3% and 19.2, respectively; also, derivatives **5** and **6** increased late apoptosis from 0.1 to 14.8% and 12.6 to 0.3%, respectively, when stained with annexin-5/PI in T-47D and MOLT4 cells compared to the control group treated with DMSO. These investigated that compounds **5** and **6** preferred the apoptotic pathway over the necrotic pathway for cell death (Fig. 4 and 5).

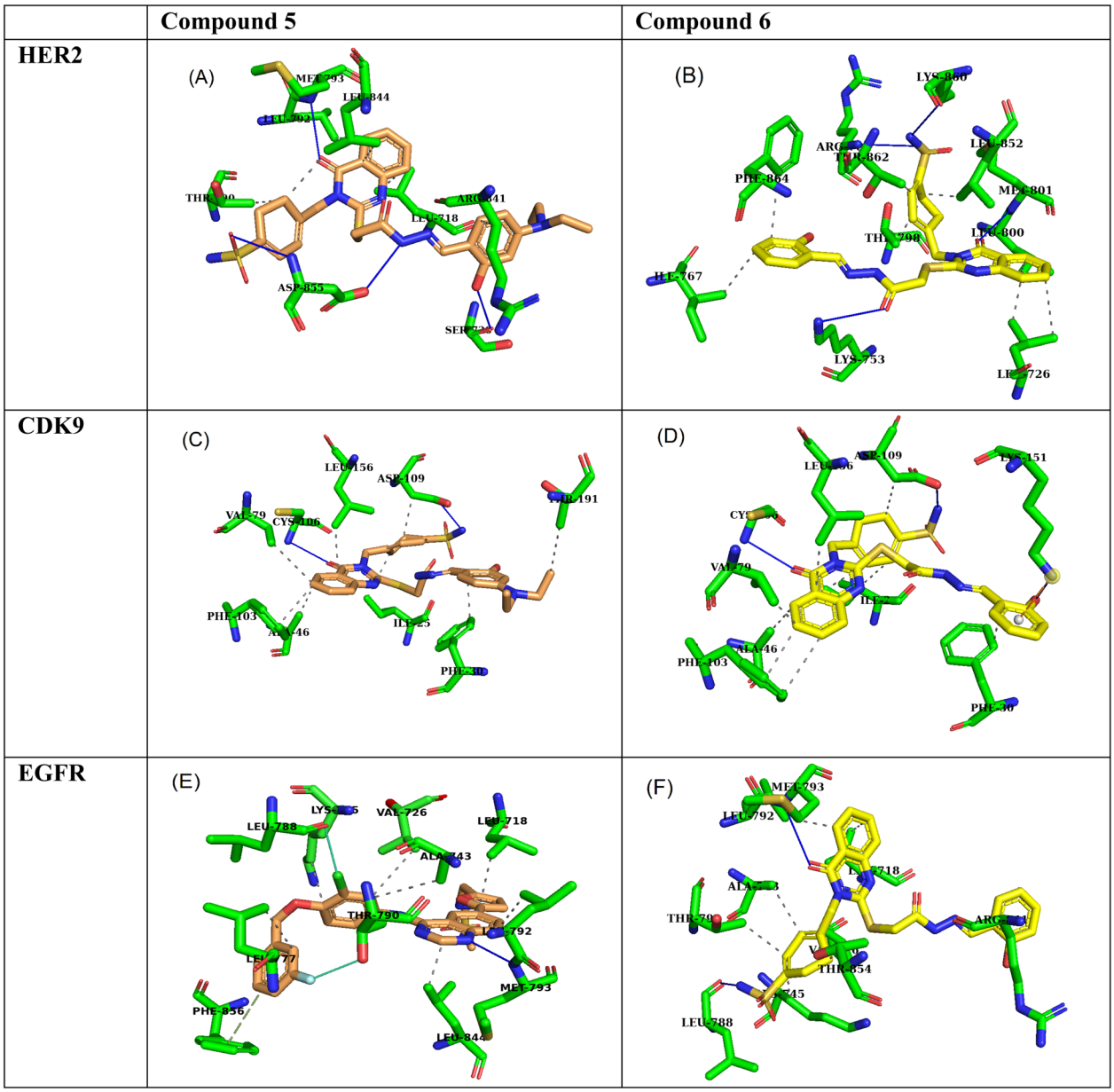

Fig. 6 3D interaction poses of compound **5** and compound **6** within the active sites of (A and B) HER2, (C and D) EGFR, and (E and F) CDK9. Compound **5** is depicted in orange, and compound **6** is in yellow.

2.5 Molecular docking

Molecular docking simulations of compound **5** and compound **6** with the HER2 receptor (PDB: 7PCD), EGFR kinase domain (PDB: 1XKK), and CDK9 (PDB: 3RCD) reveal significant insights into their potential as inhibitors, highlighting key hydrogen bond and hydrophobic interactions contributing to their binding affinities.

2.6 HER2 receptor interactions

Compound **5** exhibits a strong binding affinity of −9.2 kcal-mol^{-1} with the HER2 receptor, attributed to a network of interactions within the active site (Table 7). It forms hydrogen bonds with PHE864, LYS753, THR862, and MET801 as an acceptor and LEU796 as a donor. These hydrogen bonds, particularly those with THR862 and MET801 within the critical ATP-binding pocket, likely underpin its strong affinity. Additionally, compound **5** engages in hydrophobic interactions with LEU726, VAL734, ALA751, LYS753, GLU770, ALA771, THR798, LEU800, and PHE864, further stabilizing its binding within the hydrophobic environment of the active site (Fig. 6A). Compound **6** shows a weaker binding affinity of −7.9 kcal-mol^{-1}, forming fewer hydrogen bonds within the active site. It acts as a hydrogen bond acceptor with MET801, LYS753, LYS860, and ARG784. While the interaction with MET801 in the ATP-binding site is promising, the fewer hydrogen bonds suggest a weaker overall interaction than compound **5**. Derivative **6** also benefits from hydrophobic interactions with LEU726, ILE767, THR798, LEU800, THR862, and PHE864, contributing to its binding stability (Fig. 6B).

2.7 EGFR kinase domain interactions

Compound **5** demonstrates a strong binding affinity of −8.5 kcal mol^{-1} with the EGFR kinase domain, engaging in a network of hydrogen bonds and hydrophobic interactions within the active site (Table 7). It forms hydrogen bonds with ASP855 as both a donor and acceptor, SER720 as a donor, and MET793 as an acceptor. The interaction with MET793, a key residue within the hinge region of the ATP-binding pocket, is particularly noteworthy. Moreover, compound **5** engages in hydrophobic interactions with LEU718, THR790, LEU792, ARG841, and LEU844, further enhancing its binding stability within the hydrophobic environment of the active site (Fig. 6C).

Quinazoline **6** exhibits a slightly weaker binding affinity of −8.1 kcal mol^{-1}, forming fewer hydrogen bonds within the active site. It acts as a hydrogen bond donor with LEU788 and an acceptor with MET793. The interaction with MET793 in the ATP-binding pocket is favorable, but the lower number of hydrogen bonds suggests a slightly weaker interaction than compound **5**. Schiff base **6** also benefits from hydrophobic interactions with a broader range of residues, including LEU718, VAL726, ALA743, LYS745, THR790, LEU792, ARG841, and THR854, contributing to its overall binding stability (Fig. 6D).

2.8 CDK9 kinase interactions

Derivative **5** exhibits a binding affinity of −7.4 kcal mol^{-1} with CDK9, primarily driven by two key hydrogen bonds. It acts as a hydrogen bond acceptor with CYS106 and a donor with ASP109. These interactions likely position compound **5** within the active site to effectively interfere with ATP binding or catalytic activity. Furthermore, compound **5** benefits from hydrophobic interactions with ILE25, PHE30, ALA46, VAL79, PHE103, ASP109, LEU156, and THR191, contributing to its overall binding stability within the hydrophobic environment of the active site (Table 7, Fig. 6E). Compound **6** demonstrates a slightly stronger binding affinity of −7.7 kcal mol^{-1}, attributed to more hydrogen bonds. It forms a hydrogen bond as a donor with ASP109 and an acceptor with CYS106 and LYS151. The interaction with LYS151, while at a longer distance (4.09 Å), could provide additional binding energy. Compound **6** also engages in hydrophobic interactions with ILE25, PHE30, ALA46, VAL79, PHE103, ASP109, and LEU156, further stabilizing its binding within the active site (Fig. 6F).

3 Conclusion

The NCI, Bethesda, MD, USA, evaluated the newly synthesized quinazolines **1–13** for their *in vitro* cytotoxic activity against 59 cell lines. Acylhydrazones **5**, **6**, **7**, **9**, and **12** were the most effective at killing cancer cells, lowering the mean growth percentage (MG%) by an average of 23.5, 55.2, 89.4, 88.5, and 88.4%, in that order. Compound **5** was selected for other investigation by NCI, Bethesda, MD, USA, at five-dose dilutions on 59 tumor cells. Regarding tumor cell death, compound **5** compared to gefitinib (mean GI_{50}: 7.7 μM) and erlotinib (mean GI_{50}: 2.1 μM), with a mean GI_{50} value of 1.1 μM. It had an LC_{50} value above 100 μM, whereas the values for gefitinib and erlotinib were 95.6 μM and 14.3 μM, respectively. Those medications' TGIs were 14.3 μM and 66.3 μM, respectively, compared to compound **5**, with a TGI value of 89.2 μM. acylhydrazones **5**, **6**, **7**, **9**, and **12** exhibited the highest cytotoxic activity of the newly synthesized compounds **1–13** evaluated against the cell lines by reducing the mean growth percentage (MG%) by an average of 23.5, 55.2, 89.4, 88.5, and 88.4%, respectively. The acylhydrazones **5**, **6**, **7**, **9**, and **12** exhibit superior cytotoxic efficacy against the cell lines under investigation. The dose-dependent enzymatic inhibition experiments were conducted on EGFR, HER2, and CDK9 kinases at different dosages to determine their IC_{50} magnitudes in the nanomolar range. The Schiff base series with 2-hydroxyphenyl moiety, represented by compounds **5** and **6**, is the most effective kinase inhibitor against EGFR (IC_{50}; 84.4 and 51.5 nM), HER2 (IC_{50}; 53.9 and 44.1 nM), and CDK9 (IC_{50}; 146.9 and 96.1 nM). Compound **12** with the (3,5-dimethoxyphenyl)ethylidene)hydrazineyl) moiety demonstrated intense HER2 kinase inhibitor activity with an IC_{50} value of 110.6 nM. Schiff bases **7**, with a 3-methoxyphenyl group on the acylhydrazone moiety, demonstrated a potent CDK9 kinase inhibitor with an IC50 value of 155.4 nM. Throughout the investigation of cell cycle analysis for acylhydrazones **5** and **6**, the S phase cell count decreased from 32.3% and 9.56 in the DMSO-control cells to 20.9% in T-47D cells and 22.5% in MOLT4 cells. Additionally, compound **5** increased the proportion of T-47D cells from 6.6% in the control cell to 26.3% by halting the G2/M stage cells. After adding substance **6**, the percentage of MOLT4 cells in the G0-G1 phase decreased from 89.0% in the control cell to 61.4%. Compounds **5** and **6** enhanced early death from 0.4 and 0.6% (DMSO control sample) to 9.3% and 19.2%, respectively, as measured by flow cytometers using annexin-5/PI staining of T-47D and MOLT4 cells, respectively. The late death rate increased from 0.1 to 14.8% with derivative **5** and 12.6 to 0.3% with derivative **6**. These results demonstrate that acylhydrazones **5** and **6** preferred the apoptotic pathway than the necrotic pathway. Acylhydrazones **5** and **6** were less toxic than doxorubicin, with IC_{50} values of 45.3 and 27.8 μM, respectively, compared to 9.6 μM for doxorubicin when testing the cell death against the standard WI-38 fibroblast cell line. 2-Hydroxyacylhydrazones **5** and **6** showed potential inhibition of HER2, EGFR, and CDK9, due to their potential interaction. Due to the greater number of hydrogen bonds, 2-hydroxylamine **5** shows stronger binding affinities within the ATP-binding pockets, and the hydrophobic interactions contribute to their stability within the active sites.

4 Experimental section

4.1 Chemistry

Melting points were recorded on a Barnstead 9100 Electrothermal melting apparatus. IR spectra (KBr) were recorded on an FT-IR PerkinElmer spectrometer (n cm^{-1}). ^{1}H and ^{13}C NMR were recorded on Bruker 700 MHz spectrometers using DMSO-d_6 as the solvent. We obtained microanalytical data (C, H, and N) using a PerkinElmer 240 analyzer, and the proposed structures were within approximately 0.4% of the theoretical values.

Acquity UPLC machine (the UPH model with serial number H10UPH) and the Acquity TQD MS instrument (the TQD model with serial number QBB1203) are used for mass spectra recording. Compound **1** was prepared according to the reported method,[66] with a melting point of 301–303 °C compared to 286–287 °C.

4.2 4-((4-Oxo-2-thioxo-1,4-dihydroquinazolin-3(2*H*)-yl) methyl)benzenesulfonamide (1)

A mixture of 2-aminobenzoic acid (411 mg, 3.0 mmol) with 4-isothiocyanatobenzenesulfonamide (642.00 mg, 3.00 mmol) in ethanol (19.0 ml) and trimethylamine (404.00 mg, 4.00 mmol) was heated for 5 hours. The quinazoline-2-thione **3** was obtained by filtration, washing with iced ethanol (70%), and drying. M.p 301–303°, 90% yield; *ν*: 3203, 3134 (NH), 1777 (C=O), 1320, 1155 (O=S=O); ^{1}H NMR (700 MHz, DMSO) δ 13.15 (s, 1H), 7.97 (dd, J = 7.8, 1.6 Hz, 1H), 7.87–7.65 (m, 3H), 7.47 (dd, J = 14.4, 8.3 Hz, 3H), 7.34 (d, J = 17.8 Hz, 3H), 5.73 (s, 2H). ^{13}C NMR (176 MHz, DMSO) δ 175.89, 160.07, 143.09, 141.21, 140.08, 136.10, 127.81, 127.68, 126.15, 125.01, 116.57, 116.00, 49.11; Ms; [M+1, 348].

4.2.1 Ethyl 2-((4-oxo-3-(4-sulfamoylbenzyl)-3,4-dihydroquinazolin-2-yl)thio)acetate (2). A mixture of (695.0 mg, 2.00 mmol) 4-((4-oxo-2-thioxo-1,4-dihydroquinazolin-3(2*H*)-yl)methyl)benzenesulfonamide (**1**), (351.0 mg, 2.10 mmol) ethyl 2-bromoacetate in propane-2-one (13.0 ml) with potassium carbonate (290.0 mg, 2.10 mmol) was heated in ethanol for 6 hours. The ester **3** was obtained by filtration, washing with iced ethanol (70%), and drying. M.p 189–190°, 92% yield; *ν*: 3334, 3243 (NH), 1741, 1678 (C=O), 1340, 1154 (O=S=O); ^{1}H NMR (700 MHz, DMSO) δ 8.12 (dd, J = 8.0, 1.5 Hz, 1H), 7.87–7.79 (m, 3H), 7.52–7.33 (m, 6H), 5.42 (s, 2H), 4.14 (q, J = 7.1 Hz, 2H), 4.11 (s, 2H), 1.21 (t, J = 7.1 Hz, 3H). ^{13}C NMR (176 MHz, DMSO) δ 168.63, 161.24, 156.43, 147.14, 143.78, 139.91, 135.60, 127.57, 127.19, 126.81, 126.51, 126.34, 119.11, 61.61, 47.15, 34.67, 14.62; Ms; [M+1, 434].

4.2.2 4-((2-((2-Hydrazineyl-2-oxoethyl)thio)-4-oxoquinazolin-3(4*H*)-yl)methyl)benzenesulfonamide (3). A mixture of (867 mg, 2.0 mmol) ethyl 2-((4-oxo-3-(4-sulfamoylbenzyl)-3,4-dihydroquinazolin-2-yl)thio)acetate (**2**) and hydrazine hydrate (96 mg, 3.0 mmol), was heated in ethanol for 8 hours. The acid hydrazide **3** was obtained by filtration, washing with iced ethanol (70%), and drying. M.p 220–221°, 91% yield; *ν*: 3288, 3182, 3135 (NH), 1654, 1603 (C=O), 1329, 1159 (O=S=O); ^{1}H NMR (700 MHz, DMSO) δ 9.40 (s, 1H), 8.13 (d, J = 7.9 Hz, 1H), 7.86–7.84 (m, 1H), 7.81 (d, J = 8.1 Hz, 2H), 7.61 (d, J = 8.2 Hz, 1H), 7.50 (t, J = 7.6 Hz, 1H), 7.46 (d, J = 8.0 Hz, 2H), 7.37 (s, 2H), 5.42 (s, 2H), 4.38 & 4.32 (ss, 2H), 3.97 (s, 2H), ^{13}C NMR (176 MHz, DMSO) δ 166.48, 161.38, 156.62, 147.26, 143.65, 140.06, 135.47, 127.57, 127.11, 126.70, 126.62, 126.53, 119.14, 47.08, 34.68; Ms; [M+1, 420].

4.2.3 4-((2-((2-(Substituted-2-benzylidenehydrazineyl)-2-oxoethyl)thio)-4-oxoquinazolin-3(4*H*)-yl)methyl)benzenesulfonamide (4–9). An equimolar mixture of (210.0 mg, 0.5 mmol) 4-((2-((2-hydrazineyl-2-oxoethyl)thio)-4-oxoquinazolin-3(4H)-yl) methyl)benzenesulfonamide (**3**)and appropriate aldehyde (0.05 mmol) was heated in ethanol for 9 hours. The aldimine **4–9** was obtained by filtration, washing with iced ethanol (70%), and drying.

4.2.3.1 4-((2-((2-(2-Benzylidenehydrazineyl)-2-oxoethyl)thio)-4-oxoquinazolin-3(4H)-yl)methyl)benzenesulfonamide (4). M.p 267–268°, 93% yield; *ν*: 3363, 3249 (NH), 1667, 1602 (C=O), 1333, 1152 (O=S=O); ^{1}H NMR (500 MHz, DMSO) δ 11.85 & 11.68 (s, 1H), 8.28 & 8.08 (s, 1H), 8.12 (dd, J = 7.9, 1.7 Hz, 1H), 7.83–7.78 (m, 3H), 7.71 (td, J = 6.2, 2.0 Hz, 2H), 7.57–7.41 (m, 6H), 7.37 (d, J = 2.2 Hz, 2H), 5.45 (d, J = 3.0 Hz, 2H), 4.60 & 4.12 (s, 2H). ^{13}C NMR (176 MHz, DMSO) δ 169.10, 163.89, 161.33, 161.31, 156.85, 156.70, 147.22, 147.15, 143.91, 143.70, 143.65, 140.08, 140.03, 135.52, 134.57, 134.54, 130.61, 130.42, 129.31, 127.63, 127.60, 127.58, 127.33, 127.17, 126.74, 126.67, 126.53, 126.49, 126.47, 126.43, 119.17, 119.12, 47.18, 35.61, 34.49; Ms; [M+1, 508].

4.2.3.2 4-((2-((2-(2-(4-(Diethylamino)-2-hydroxybenzylidene) hydrazineyl)-2-oxoethyl)thio)-4-oxoquinazolin-3(4H)-yl)methyl) benzenesulfonamide (5). M.p 270–271°, 92% yield; *ν*: 3429 (OH), 3303, 3201 (NH), 1780, 1636 (C=O), 1331, 1153 (O=S=O); ^{1}H NMR (700 MHz, DMSO) δ 11.76 & 11.36 (s, 1H), 11.14 & 9.98 (s, 1H), 8.25 & 8.16 (s, 1H), 8.12 (ddd, J = 8.3, 4.4, 1.6 Hz, 1H), 7.85–7.76 (m, 3H), 7.59–7.53 (m, 1H), 7.51–7.44 (m, 3H), 7.40–7.32 (m, 2H), 7.21 (d, J = 8.8 Hz, 1H), 6.25 & 6.18 (dd, J = 8.8, 2.5 Hz, 1H), 6.12 & 6.08 (d, J = 2.4 Hz, 1H), 5.43 (d, J = 5.8 Hz, 2H), 4.50 (s, 1H), 4.08 (s, 1H), 3.35–3.31 (m, 4H), 1.10–1.07 (m, 6H), ^{13}C NMR (176 MHz, DMSO) δ 167.18, 162.34, 160.79, 159.42, 158.26, 156.35, 156.14, 150.09, 149.97, 148.74, 146.71, 146.69, 143.14, 143.07, 139.55, 139.48, 134.99, 134.96, 131.38, 127.10, 127.04, 126.64, 126.60, 126.20, 126.11, 125.99, 125.95, 125.93, 125.91, 118.62, 118.58, 107.04, 106.11, 103.86, 103.59, 97.29, 97.16, 46.61, 43.74, 43.71, 34.80, 34.29, 12.44; Ms; [M+1, 595].

4.2.3.3 4-((2-((2-(2-(2-Hydroxybenzylidene)hydrazineyl)-2-oxoethyl)thio)-4-oxoquinazolin-3(4H)-yl)methyl)benzenesulfonamide (6). M.p 288–290°, 94% yield; *ν*: 3372, 3265, 3183 (NH), 1671, 1611 (C=O), 1338, 1156 (O=S=O); ^{1}H NMR (500 MHz, DMSO) δ 11.80 & 11.62 (s, 1H), 9.66 (s, 1H), 8.17 & 8.00 (s, 1H), 8.13–8.10 (m, 1H), 7.85–7.76 (m, 3H), 7.59–7.43 (m, 4H), 7.38 (d, J = 2.7 Hz, 2H), 7.28–7.06 (m, 3H), 6.84–6.82 (m, 1H), 5.45 (d, J = 5.8 Hz, 2H), 4.58 & 4.10 (s, 2H); ^{13}C NMR (176 MHz, DMSO) δ 168.74, 163.87, 161.35, 161.33, 157.70, 156.89, 156.84, 156.62, 147.37, 147.21, 143.67, 143.62, 141.63, 140.10, 140.02, 135.55, 135.52, 131.97, 131.72, 129.63, 127.65, 127.59, 127.18, 127.16, 126.84, 126.78, 126.69, 126.54, 126.50, 126.46, 126.42, 120.51, 119.91, 119.88, 119.15, 119.10, 116.82, 116.64, 47.19, 35.34, 34.61; Ms; [M+1, 524].

4.2.3.4 4-((2-((2-(2-(3-Methoxybenzylidene)hydrazineyl)-2-oxoethyl)thio)-4-oxoquinazolin-3(4H)-yl)methyl)benzenesulfonamide (7). M.p 279–280°, 91% yield; *ν*: 3362, 3246 (NH), 1669, 1590 (C=O), 1351, 1151 (O=S=O); ^{1}H NMR (500 MHz, DMSO) δ 11.86 & 11.70 (s, 1H), 8.24 & 8.05 (s, 1H), 8.12 (dt, J = 8.0, 2.0 Hz, 1H), 7.80 (qd, J = 7.9, 1.6 Hz, 3H), 7.56–7.43 (m, 4H), 7.37 (q, J = 2.4 Hz, 2H), 7.35–7.25 (m, 3H), 7.03–6.98 (m, 1H), 5.45 (d, J = 3.9 Hz, 2H), 4.61& 4.12 (s, 2H), 3.79 (d, J = 2.6 Hz, 3H), ^{13}C NMR (176 MHz, DMSO) δ 169.10, 163.94, 161.33, 161.30, 160.01, 159.98, 156.86, 156.69, 147.21, 147.03, 143.76, 143.69, 143.65, 140.08, 140.03, 136.00, 135.96, 135.53, 135.50, 130.43, 127.63,

127.61, 127.17, 126.74, 126.66, 126.53, 126.50, 126.47, 126.39, 120.47, 119.93, 119.16, 119.12, 116.78, 116.33, 112.01, 111.70, 55.64, 55.60, 49.08, 47.18, 35.59, 34.57; Ms; [M+1, 538].

*4.2.3.5 4-((4-Oxo-2-((2-oxo-2-(2-(3,4,5-trimethoxybenzylidene) hydrazineyl)ethyl)thio)quinazolin-3(4H)-yl)methyl)benzenesulfonamide (**8**).* M.p 210–212°, 91% yield; *ν*: 3300, 3249 (NH), 1655, 1611 (C═O), 1331, 1149 (O═S═O); ^{1}H NMR (700 MHz, DMSO) δ 11.82 & 11.71 (ss, 1H), 9.39 (s, 1H), 8.13 (d, J = 7.7 Hz, 1H), 7.89–7.78 (m, 3H), 7.65–7.59 (m, 1H), 7.52–7.45 (m, 3H), 7.36 (s, 2H), 7.07–6.98 (m, 1H), 6.79 (s, 1H), 5.47–5.39 (m, 2H), 4.50–4.11 (m, 2H), 4.69–3.66 (m, 9H); ^{13}C NMR (176 MHz, DMSO) δ 166.47, 161.38, 156.64, 153.64, 153.48, 147.27, 143.66, 140.06, 138.67, 137.51, 135.47, 132.58, 127.57, 127.12, 126.70, 126.62, 126.52, 119.15, 106.06, 104.78, 104.58, 102.73, 60.50, 56.42, 56.35, 56.18, 47.07, 34.69; \Ms; [M+1, 598].

*4.2.3.6 4-((2-((2-(2-(4-Methylbenzylidene)hydrazineyl)-2-oxoethyl)thio)-4-oxoquinazolin-3(4H)-yl)methyl)benzenesulfonamide (**9**).* M.p 273–274°, 95% yield; *ν*: 3302, 3236 (NH), 1665, 1610 (C═O), 1334, 1153 (O═S═O); ^{1}H NMR (700 MHz, DMSO) δ 11.77 & 11.61 (s, 1H), 8.23 & 8.04 (s, 1H), 8.13–8.12 (m, 1H), 7.84–7.79 (m, 3H), 7.61–7.46 (m, 6H), 7.36 (s, 2H), 7.27–7.23 (m, 2H), 5.45 (d, J = 4.5 Hz, 2H), 4.59 & 4.11 (s, 2H), 2.34 (s, 3H); ^{13}C NMR (176 MHz, DMSO) δ 168.95, 163.73, 161.34, 161.31, 156.88, 156.71, 147.23, 143.99, 143.66, 140.21, 140.08, 135.51, 131.85, 129.91, 127.63, 127.59, 127.56, 127.31, 127.17, 126.66, 126.53, 126.49, 126.47, 119.13, 47.18, 35.61, 34.52, 21.50; Ms; [M+1, 522].

4.2.4 4-((4-Oxo-2-((2-oxo-2-(2-(1-(substituted-phenyl)ethylidene)hydrazineyl)ethyl)thio)quinazolin-3(4*H*)-yl)methyl)benzenesulfonamide (10–13). An equimolar mixture of (210.0 mg, 0.5 mmol) 4-((2-((2-hydrazineyl-2-oxoethyl)thio)-4-oxoquinazolin-3(4H)-yl)methyl)benzenesulfonamide (**3**) and appropriate ketone (0.05 mmol) was heated in ethanol for 11.0 hours. The ketimine **4–13** was obtained by filtration, washing with iced ethanol (70%), and drying.

*4.2.4.1 4-((4-Oxo-2-((2-oxo-2-(2-(1-(p-tolyl)ethylidene)hydrazineyl)ethyl)thio)quinazolin-3(4H)-yl)methyl)benzenesulfonamide (**10**).* M.p 279–280°, 90% yield; *ν*: 3353, 3201 (NH), 1668, 1610 (C═O), 1338, 1156 (O═S═O); ^{1}H NMR (700 MHz, DMSO) δ 10.93 & 10.80 (s, 1H), 8.13 (t, J = 9.3 Hz, 1H), 7.84–7.78 (m, 5H), 7.61–7.38 (m, 9H), 5.45 & 5.42 (s, 2H), 4.65 (d, J = 3.1 Hz, 1.3H), 4.25 (d, J = 3.2 Hz, 0.7H), 2.33 (s, 1H), 2.30 (d, J = 2.7 Hz, 2H), ^{13}C NMR (176 MHz, DMSO) δ 169.96, 161.35, 156.92, 152.64, 148.52, 147.26, 147.23, 143.68, 143.63, 140.09, 140.05, 138.45, 135.55, 129.84, 129.66, 128.87, 128.81, 127.62, 127.57, 127.17, 126.81, 126.66, 126.56, 126.49, 126.40, 119.12, 47.15, 35.52, 35.20, 14.71, 14.15; Ms; [M+1, 522].

*4.2.4.2 4-((2-((2-(2-(1-(3-Methoxyphenyl)ethylidene)hydrazineyl)-2-oxoethyl)thio)-4-oxoquinazolin-3(4H)-yl)methyl)benzenesulfonamide (**11**).* M.p 263–265°, 88% yield; *ν* 3356, 3255, 3200 (NH), 17 674, 1619 (C═O), 133, 1157 (O═S═O); ^{1}H NMR (700 MHz, DMSO) δ 10.95 & 10.80 (s, 1H), 8.13 (t, J = 9.5 Hz, 1H), 7.83 (td, J = 17.3, 7.5 Hz, 3H), 7.59–7.29 (m, 9H), 7.00 (d, J = 7.9 Hz, 1H), 5.46 (s, 2H), 4.67 & 4.25 (s, 2H), 3.78 (s, 3H), 2.32 & 2.29 (s, 3H); ^{13}C NMR (176 MHz, DMSO) δ 169.97, 161.35, 159.74, 159.65, 156.94, 156.90, 148.31, 147.25, 143.70, 143.64, 140.10, 140.05, 139.93, 135.52, 129.96, 129.88, 127.59, 126.51, 126.40, 119.35, 119.13, 119.07, 115.42, 115.01, 112.20, 112.14, 55.59, 47.18, 35.44, 14.88, 14.27; Ms; [M+1, 552].

*4.2.4.3 4-((2-((2-(2-(1-(3,5-Dimethoxyphenyl)ethylidene)hydrazineyl)-2-oxoethyl)thio)-4-oxoquinazolin-3(4H)-yl)methyl)benzenesulfonamide (**12**).* M.p 295–296°, 89% yield; *ν*: 3331, 3261 (NH), 1674, 1591 (C═O), 1336, 1158 (O═S═O); ^{1}H NMR (700 MHz, DMSO) δ 10.95 & 10.80 (s, 1H), 8.13 (dd, J = 12.3, 7.4 Hz, 1H), 7.84–7.79 (m, 3H), 7.48 (td, J = 15.1, 7.1 Hz, 4H), 7.38 (d, J = 4.0 Hz, 2H), 6.99 & 6.92 (s, 2H), 6.62–6.51 (m, 1H), 5.45 (s, 2H), 4.66 & 4.24 (s, 2H), 3.77 (d, J = 2.9 Hz, 6H), 2.30 (s, 1H), 2.27 (d, J = 2.7 Hz, 2H), ^{13}C NMR (176 MHz, DMSO) δ 169.97, 160.88, 160.77, 156.94, 148.27, 147.24, 143.62, 140.53, 140.10, 135.48, 127.63, 127.58, 127.15, 126.66, 126.51, 126.38, 119.11, 105.02, 104.97, 101.63, 101.17, 55.73, 47.18, 35.56, 35.48, 14.95, 14.31; Ms; [M+1, 582].

*4.2.4.4 4-((4-Oxo-2-((2-oxo-2-(2-(1-(3,4,5-trimethoxyphenyl) ethylidene)hydrazineyl)ethyl)thio)quinazolin-3(4H)-yl)methyl)benzenesulfonamide (**13**).* M.p 283–284°, 90% yield; *ν*: 3322, 3243, 3168 (NH), 1659, 1612 (C═O), 1333, 1162 (O═S═O); ^{1}H NMR (700 MHz, DMSO) δ 10.91 & 10.77 (t, J = 4.2 Hz, 1H), 8.13 (p, J = 6.7 Hz, 1H), 7.90–7.79 (m, 3H), 7.59–7.42 (m, 4H), 7.39–7.38 (m, 2H), 7.13–7.06 (m, 2H), 5.46 (s, 2H), 4.66 & 4.24 (t, J = 4.1 Hz, 2H), 3.81 (s, 6H), 3.70 (s, 3H), 2.34–2.30 (m, 3H); ^{13}C NMR (176 MHz, DMSO) δ 169.81, 164.22, 161.34, 156.99, 156.91, 153.16, 153.09, 148.60, 147.25, 143.64, 140.10, 139.17, 135.52, 134.08, 133.99, 127.65, 127.55, 127.19, 126.67, 126.52, 126.35, 119.11, 104.41, 104.31, 60.60, 56.38, 47.20, 35.56, 15.00, 14.36; Ms; [M+1, 612].

4.3 Biological evaluation

4.3.1 *In vitro* cytotoxic activity. The *in vitro* cytotoxicity assay was evaluated following the protocol of the Drug Evaluation Branch, National Cancer Institute, Bethesda, MD[66,67] ESI.†

4.3.2 *In vitro* cyclooxygenase (COX) inhibition assay. The colorimetric COX (ovine) inhibitor screening assay kit (kit catalog number 560101, Cayman Chemical, Ann Arbor, MI) was utilized according to the manufacturer's instructions to examine the ability of the test compounds and the reference drug to inhibit the COX-2 isozymes[68,69] ESI.†

4.3.3 Kinases assay. *In vitro* luminescent EGFR tyrosine kinase assay using Kinase-Glo® MAX as a detection reagent[70] and *In vitro* HER2 tyrosine kinase assay using DP-Glo™ reagent[71,72] that measures ADP formed from a kinase reaction, this luminescent signal positively correlates with ADP amount and kinase activity. *In vitro*, luminescent CDK9 kinase assay using Kinase-Glo® MAX as a detection reagent[73] ESI.†

4.4 Apoptosis assay

The apoptosis of cancer cell lines T-47D and MOLT4 cells was measured by Annexin 5-FITC/PI apoptosis detection kit using FACSCalibur flow cytometer for analysis[74] ESI.†

4.5 Cell cycle analysis

Cancer cell lines T-47D and MOLT4 were stained with the DNA fluorochrome PI and analyzed by FACSCalibur flow cytometer.[75]

4.6 Docking methodology

We performed molecular docking simulations using AutoDock 4.2,[76] which employed the Lamarckian Genetic Algorithm (LGA) with defined parameters. We used Accelrys Discovery Studio Visualizer (version 4.0) to visualize binding poses and interactions and analyze the binding dynamics. We further characterized intermolecular interactions using the PLIP web server.[77–82]

Data availability

Data supporting this study are included in the article and ESI.†

Conflicts of interest

The authors declare that they have no conflict of interest.

Acknowledgements

The authors extend their appreciation to the Researchers Supporting Project number (RSPD2024R1049), King Saud University, Riyadh, Saudi Arabia, for funding this research.

References

1 M. Mareel and A. J. P. r. Leroy, Clinical, cellular, and molecular aspects of cancer invasion, *Physiol. Rev.*, 2003, **83**, 337–376.
2 J. Wesche, K. Haglund and E. M. J. B. J. Haugsten, Fibroblast growth factors and their receptors in cancer, *Biochem. J.*, 2011, **437**, 199–213.
3 J. Ferlay, M. Ervik, F. Lam, M. Colombet, L. Mery, M. Piñeros, A. Znaor, I. Soerjomataram and F. J. L. I. a. f. r. o. c. Bray, *Global Cancer Observatory: Cancer Today*, 2020, 20182020.
4 A. M. Alanazi, I. A. Al-Suwaidan, A.-M. Alaa, M. A. Mohamed, A. M. El_Morsy and A. S. El-Azab, Design, synthesis and biological evaluation of some novel substituted 2-mercapto-3-phenethylquinazolines as antitumor agents, *Med. Chem. Res.*, 2013, **22**, 5566–5577.
5 A. S. El-Azab, A. A. Abdel-Aziz, H. A. Ghabbour and M. A. Al-Gendy, Synthesis, in vitro antitumour activity, and molecular docking study of novel 2-substituted mercapto-3-(3,4,5-trimethoxybenzyl)-4(3H)-quinazolinone analogues, *J. Enzyme Inhib. Med. Chem.*, 2017, **32**, 1229–1239.
6 A. M. Alanazi, A. A.-M. Abdel-Aziz, T. Z. Shawer, R. R. Ayyad, A. M. Al-Obaid, M. H. Al-Agamy, A. R. Maarouf and A. S. El-Azab, Synthesis, antitumor and antimicrobial activity of some new 6-methyl-3-phenyl-4 (3 H)-quinazolinone analogues: in silico studies, *J. Enzyme Inhib. Med. Chem.*, 2016, **31**, 721–735.
7 A. M. Alanazi, A.-M. Alaa, I. A. Al-Suwaidan, S. G. Abdel-Hamide, T. Z. Shawer and A. S. El-Azab, Design, synthesis and biological evaluation of some novel substituted quinazolines as antitumor agents, *Eur. J. Med. Chem.*, 2014, **79**, 446–454.
8 J.-H. Cheng, C.-F. Hung, S.-C. Yang, J.-P. Wang, S.-J. Won and C.-N. Lin, Synthesis and cytotoxic, anti-inflammatory, and anti-oxidant activities of 2′, 5′-dialkoxylchalcones as cancer chemopreventive agents, *Bioorg. Med. Chem.*, 2008, **16**, 7270–7276.
9 A.-M. Alaa, L. A. Abou-Zeid, K. E. H. ElTahir, M. A. Mohamed, M. A. A. El-Enin and A. S. El-Azab, Design, synthesis of 2, 3-disubstitued 4 (3H)-quinazolinone derivatives as anti-inflammatory and analgesic agents: COX-1/2 inhibitory activities and molecular docking studies, *Bioorg. Med. Chem.*, 2016, **24**, 3818–3828.
10 A. A. Abdel-Aziz, L. A. Abou-Zeid, K. E. H. ElTahir, R. R. Ayyad, M. A. El-Sayed and A. S. El-Azab, Synthesis, anti-inflammatory, analgesic, COX-1/2 inhibitory activities and molecular docking studies of substituted 2-mercapto-4(3H)-quinazolinones, *Eur. J. Med. Chem.*, 2016, **121**, 410–421.
11 A.-M. Alaa, L. A. Abou-Zeid, K. E. H. ElTahir, R. R. Ayyad, A.-A. Magda and A. S. El-Azab, Synthesis, anti-inflammatory, analgesic, COX-1/2 inhibitory activities and molecular docking studies of substituted 2-mercapto-4 (3H)-quinazolinones, *Eur. J. Med. Chem.*, 2016, **121**, 410–421.
12 A.-M. Alaa, L. A. Abou-Zeid, K. E. H. ElTahir, M. A. Mohamed, M. A. A. El-Enin and A. S. El-Azab, Design, synthesis of 2, 3-disubstitued 4 (3H)-quinazolinone derivatives as anti-inflammatory and analgesic agents: COX-1/2 inhibitory activities and molecular docking studies, *Bioorg. Med. Chem.*, 2016, **24**, 3818–3828.
13 A. S. El-Azab, A. A. Abdel-Aziz, S. Bua, A. Nocentini, M. A. El-Gendy, M. A. Mohamed, T. Z. Shawer, N. A. AlSaif and C. T. Supuran, Synthesis of benzensulfonamides linked to quinazoline scaffolds as novel carbonic anhydrase inhibitors, *Bioorg. Chem.*, 2019, **87**, 78–90.
14 A. S. El-Azab, A. A. Abdel-Aziz, H. E. A. Ahmed, S. Bua, A. Nocentini, N. A. AlSaif, A. J. Obaidullah, M. M. Hefnawy and C. T. Supuran, Exploring structure-activity relationship of S-substituted 2-mercaptoquinazolin-4(3H)-one including 4-ethylbenzenesulfonamides as human carbonic anhydrase inhibitors, *J. Enzyme Inhib. Med. Chem.*, 2020, **35**, 598–609.
15 A. S. El-Azab, A. A. Abdel-Aziz, S. Bua, A. Nocentini, N. A. AlSaif, M. M. Alanazi, M. A. El-Gendy, H. E. A. Ahmed and C. T. Supuran, S-substituted 2-mercaptoquinazolin-4(3H)-one and 4-ethylbenzensulfonamides act as potent and selective human carbonic anhydrase IX and XII inhibitors, *J. Enzyme Inhib. Med. Chem.*, 2020, **35**, 733–743.
16 A. S. El-Azab, A. A.-M. Abdel-Aziz, S. Bua, A. Nocentini, N. A. AlSaif, M. M. Alanazi, M. A. El-Gendy, H. E. Ahmed and C. T. Supuran, S-substituted 2-mercaptoquinazolin-4 (3H)-one and 4-ethylbenzensulfonamides act as potent and selective human carbonic anhydrase IX and XII inhibitors, *J. Enzyme Inhib. Med. Chem.*, 2020, **35**, 733–743.
17 A. S. El-Azab, A.-M. Alaa, S. Bua, A. Nocentini, M. A. El-Gendy, M. A. Mohamed, T. Z. Shawer, N. A. AlSaif and C. T. Supuran, Synthesis of benzensulfonamides linked to quinazoline scaffolds as novel carbonic anhydrase inhibitors, *Bioorg. Chem.*, 2019, **87**, 78–90.

18 A. S. El-Azab, A. Al-Dhfyan, A. A. Abdel-Aziz, L. A. Abou-Zeid, H. M. Alkahtani, A. M. Al-Obaid and M. A. Al-Gendy, Synthesis, anticancer and apoptosis-inducing activities of quinazoline-isatin conjugates: epidermal growth factor receptor-tyrosine kinase assay and molecular docking studies, *J. Enzyme Inhib. Med. Chem.*, 2017, **32**, 935–944.

19 H. M. Alkahtani, A. N. Abdalla, A. J. Obaidullah, M. M. Alanazi, A. A. Almehizia, M. G. Alanazi, A. Y. Ahmed, O. I. Alwassil, H. W. Darwish, A. A. Abdel-Aziz and A. S. El-Azab, Synthesis, cytotoxic evaluation, and molecular docking studies of novel quinazoline derivatives with benzenesulfonamide and anilide tails: Dual inhibitors of EGFR/HER2, *Bioorg. Chem.*, 2020, **95**, 103461.

20 A. J. Barker, K. H. Gibson, W. Grundy, A. A. Godfrey, J. J. Barlow, M. P. Healy, J. R. Woodburn, S. E. Ashton, B. J. Curry, L. Scarlett, L. Henthorn and L. Richards, Studies leading to the identification of ZD1839 (IRESSA): an orally active, selective epidermal growth factor receptor tyrosine kinase inhibitor targeted to the treatment of cancer, *Bioorg. Med. Chem. Lett.*, 2001, **11**, 1911–1914.

21 R. T. Dungo and G. M. Keating, Afatinib: first global approval, *Drugs*, 2013, **73**, 1503–1515.

22 J. E. Frampton, Lapatinib: a review of its use in the treatment of HER2-overexpressing, trastuzumab-refractory, advanced or metastatic breast cancer, *Drugs*, 2009, **69**, 2125–2148.

23 A. S. El-Azab, A. A. Abdel-Aziz, N. A. AlSaif, H. M. Alkahtani, M. M. Alanazi, A. J. Obaidullah, R. O. Eskandrani and A. Alharbi, Antitumor activity, multitarget mechanisms, and molecular docking studies of quinazoline derivatives based on a benzenesulfonamide scaffold: Cell cycle analysis, *Bioorg. Chem.*, 2020, **104**, 104345.

24 A. Hamdi, H. W. El-Shafey, D. I. Othman, A. S. El-Azab, N. A. AlSaif and A.-M. J. B. C. Alaa, *Design, synthesis, antitumor, and VEGFR-2 inhibition activities of novel 4-anilino-2-vinyl-quinazolines: Molecular modeling studies*, 122 (2022).

25 A. S. Altamimi, A. S. El-Azab, S. G. Abdelhamid, M. A. Alamri, A. H. Bayoumi, S. M. Alqahtani, A. B. Alabbas, A. I. Altharawi, M. A. Alossaimi and M. A. J. M. Mohamed, *Synthesis, anticancer screening of some novel trimethoxy quinazolines and VEGFR2, EGFR tyrosine kinase inhibitors assay; molecular docking studies*, 26 (2021) 2992.

26 A. S. El-Azab, A.-M. Alaa, N. A. AlSaif, H. M. Alkahtani, M. M. Alanazi, A. J. Obaidullah, R. O. Eskandrani, A. J. B. C. Alharbi, *Antitumor activity, multitarget mechanisms, and molecular docking studies of quinazoline derivatives based on a benzenesulfonamide scaffold: Cell cycle analysis*, 104 (2020).

27 M. A.-A. El-Sayed, W. M. El-Husseiny, N. I. Abdel-Aziz, A. S. El-Azab, H. A. Abuelizz and A. A.-M. Abdel-Aziz, Synthesis and biological evaluation of 2-styrylquinolines as antitumour agents and EGFR kinase inhibitors: molecular docking study, *J. Enzyme Inhib. Med. Chem.*, 2018, **33**, 199–209.

28 A. S. El-Azab, S. G. Abdel-Hamide, M. M. Sayed-Ahmed, G. S. Hassan, T. M. El-Hadiyah, O. A. Al-Shabanah, O. A. Al-Deeb and H. I. El-Subbagh, Novel 4 (3 H)-quinazolinone analogs: synthesis and anticonvulsant activity, *Med. Chem. Res.*, 2013, **22**, 2815–2827.

29 A. S. El-Azab, K. E. J. B. ElTahir and M. C. Letters, *Design and synthesis of novel 7-aminoquinazoline derivatives: Antitumor and anticonvulsant activities*, 22 (2012) 1879–1885.

30 A. S. El-Azab and K. E. ElTahir, Synthesis and anticonvulsant evaluation of some new 2, 3, 8-trisubstituted-4 (3H)-quinazoline derivatives, *Bioorg. Med. Chem. Lett.*, 2012, **22**, 327–333.

31 A. S. El-Azab, K. E. ElTahir and S. M. Attia, Synthesis and anticonvulsant evaluation of some novel 4 (3H)-quinazolinones, *Monatsh. fur Chem.*, 2011, **142**, 837–848.

32 A. S. El-Azab, A. A.-M. Abdel-Aziz, H. A. Ghabbour and M. A. Al-Gendy, Synthesis, in vitro antitumour activity, and molecular docking study of novel 2-substituted mercapto-3-(3, 4, 5-trimethoxybenzyl)-4 (3H)-quinazolinone analogues, *J. Enzyme Inhib. Med. Chem.*, 2017, **32**, 1229–1239.

33 A. S. El-Azab, A. Al-Dhfyan, A. A.-M. Abdel-Aziz, L. A. Abou-Zeid, H. M. Alkahtani, A. M. Al-Obaid, M. A. J. J. o. E. I. Al-Gendy, M. Chemistry, *Synthesis, anticancer and apoptosis-inducing activities of quinazoline–isatin conjugates: epidermal growth factor receptor-tyrosine kinase assay and molecular docking studies*, 32 (2017) 935–944.

34 I. A. Al-Suwaidan, A. A.-M. Abdel-Aziz, T. Z. Shawer, R. R. Ayyad, A. M. Alanazi, A. M. El-Morsy, M. A. Mohamed, N. I. Abdel-Aziz, M. A.-A. El-Sayed, A. S. J. J. o. e. i. El-Azab, m. chemistry, *Synthesis, antitumor activity and molecular docking study of some novel 3-benzyl-4 (3H) quinazolinone analogues*, 31 (2016) 78–89.

35 M. A. Mohamed, R. R. Ayyad, T. Z. Shawer, A.-M. Alaa, A. S. J. E. J. O. M. C. El-Azab, *Synthesis and antitumor evaluation of trimethoxyanilides based on 4 (3H)-quinazolinone scaffolds*, 112 (2016) 106–113.

36 A. M. Alanazi, A.-M. Alaa, I. A. Al-Suwaidan, S. G. Abdel-Hamide, T. Z. Shawer, A. S. J. E. J. o. M. C. El-Azab, *Design, synthesis and biological evaluation of some novel substituted quinazolines as antitumor agents*, 79 (2014) 446–454.

37 A. M. Alanazi, I. A. Al-Suwaidan, A. A.-M. Abdel-Aziz, M. A. Mohamed, A. M. El_Morsy, A. S. J. M. C. R. El-Azab, *Design, synthesis and biological evaluation of some novel substituted 2-mercapto-3-phenethylquinazolines as antitumor agents*, 22 (2013) 5566–5577.

38 I. A. Al-Suwaidan, A. M. Alanazi, A.-M. Alaa, M. A. Mohamed, A. S. J. B. El-Azab and M. C. Letters, *Design, synthesis and biological evaluation of 2-mercapto-3-phenethylquinazoline bearing anilide fragments as potential antitumor agents: molecular docking study*, 23 (2013) 3935–3941.

39 A. S. El-Azab, M. A. Al-Omar, A.-M. Alaa, N. I. Abdel-Aziz, A.-A. Magda, A. M. Aleisa, M. M. Sayed-Ahmed and S. G. Abdel-Hamide, Design, synthesis and biological evaluation of novel quinazoline derivatives as potential antitumor agents: molecular docking study, *Eur. J. Med. Chem.*, 2010, **45**, 4188–4198.

40 A. M. Alanazi, A. A.-M. Abdel-Aziz, T. Z. Shawer, R. R. Ayyad, A. M. Al-Obaid, M. H. Al-Agamy, A. R. Maarouf and A. S. El-Azab, Synthesis, antitumor and antimicrobial activity of some new 6-methyl-3-phenyl-4 (3 H)-quinazolinone

analogues: in silico studies, *J. Enzyme Inhib. Med. Chem.*, 2016, **31**, 721–735.

41 A. M. Alafeefy, A. S. El-Azab, M. A. Mohamed, M. A. Bakhat and S. Abdel-Hamid, Synthesis of some new substituted iodoquinazoline derivatives and their antimicrobial screening, *J. Saudi Chem. Soc.*, 2011, **15**, 319–325.

42 A. S. El-Azab, Synthesis of some new substituted 2-mercaptoquinazoline analogs as potential antimicrobial agents, *Phosphorus, Sulfur Relat. Elem.*, 2007, **182**, 333–348.

43 M. Aziza, M. Nassar, S. AbdelHamide, A. ElHakim and A. El-Azab, Synthesis and antimicrobial activities of some new 3-heteroaryl-quinazolin-4-ones, *Indian J. Heterocycl. Chem.*, 1996, **6**, 25–30.

44 A. S. El-Azab, H. M. Alkahtani, N. A. AlSaif, I. A. Al-Suwaidan, A. J. Obaidullah, M. M. Alanazi, A. M. Al-Obaid, M. H. Al-Agamy, A.-M. J. J. o. M. S. Alaa, *Synthesis, antiproliferative and enzymatic inhibition activities of quinazolines incorporating benzenesulfonamide: Cell cycle analysis and molecular modeling study*, 1278 (2023).

45 A. A.-M. Abdel-Aziz, A. S. El-Azab, N. A. AlSaif, A. J. Obaidullah, A. M. Al-Obaid and I. A. Al-Suwaidan, Synthesis, potential antitumor activity, cell cycle analysis, and multitarget mechanisms of novel hydrazones incorporating a 4-methylsulfonylbenzene scaffold: a molecular docking study, *J. Enzyme Inhib. Med. Chem.*, 2021, **36**, 1520–1538.

46 G. Xu, M. C. Abad, P. J. Connolly, M. P. Neeper, G. T. Struble, B. A. Springer, S. L. Emanuel, N. Pandey, R. H. Gruninger, M. J. B. Adams, m. c. letters, *4-Amino-6-arylamino-pyrimidine-5-carbaldehyde hydrazones as potent ErbB-2/EGFR dual kinase inhibitors*, 18 (2008) 4615–4619.

47 A. A.-M. Abdel-Aziz, A. S. El-Azab, N. A. AlSaif, M. M. Alanazi, M. A. El-Gendy, A. J. Obaidullah, H. M. Alkahtani, A. A. Almehizia, I. A. J. J. o. E. I. Al-Suwaidan, M. Chemistry, *Synthesis, anti-inflammatory, cytotoxic, and COX-1/2 inhibitory activities of cyclic imides bearing 3-benzenesulfonamide, oxime, and β-phenylalanine scaffolds: a molecular docking study*, 35 (2020) 610–621.

48 A. S. El-Azab, A. A.-M. Abdel-Aziz, H. E. Ahmed, S. Bua, A. Nocentini, N. A. AlSaif, A. J. Obaidullah, M. M. Hefnawy and C. T. Supuran, Exploring structure-activity relationship of S-substituted 2-mercaptoquinazolin-4 (3H)-one including 4-ethylbenzenesulfonamides as human carbonic anhydrase inhibitors, *J. Enzyme Inhib. Med. Chem.*, 2020, **35**, 598–609.

49 H. M. Alkahtani, A. N. Abdalla, A. J. Obaidullah, M. M. Alanazi, A. A. Almehizia, M. G. Alanazi, A. Y. Ahmed, O. I. Alwassil, H. W. Darwish, A.-M. J. B. C. Alaa, *Synthesis, cytotoxic evaluation, and molecular docking studies of novel quinazoline derivatives with benzenesulfonamide and anilide tails: Dual inhibitors of EGFR/HER2*, 95 (2020).

50 A. S. El-Azab, A.-M. Alaa, S. Bua, A. Nocentini, M. M. Alanazi, N. A. AlSaif, I. A. Al-Suwaidan, M. M. Hefnawy, C. T. J. B. C. Supuran, *Synthesis and comparative carbonic anhydrase inhibition of new Schiff's bases incorporating benzenesulfonamide, methanesulfonamide, and methylsulfonylbenzene scaffolds*, 92 (2019).

51 A. S. El-Azab, A.-M. Alaa, S. Bua, A. Nocentini, N. A. AlSaif, A. A. Almehizia, M. M. Alanazi, M. M. Hefnawy and C. T. Supuran, New anthranilic acid-incorporating N-benzenesulfonamidophthalimides as potent inhibitors of carbonic anhydrases I, II, IX, and XII: Synthesis, in vitro testing, and in silico assessment, *J. Enzyme Inhib. Med. Chem.*, 2019, **181**, 111573.

52 A.-M. Alaa, A. S. El-Azab, S. Bua, A. Nocentini, M. A. A. El-Enin, M. M. Alanazi, N. A. AlSaif, M. M. Hefnawy, C. T. J. B. c. Supuran, *Design, synthesis, and carbonic anhydrase inhibition activity of benzenesulfonamide-linked novel pyrazoline derivatives*, 87 (2019) 425–431.

53 A. Abdel-Aziz, A. Angeli, A. El-Azab, M. Hammouda, M. El-sherbeny, C. J. B. C. Supuran, *Synthesis and auti-inflammatory activity of sulphonamides and carboxygenase/carbonic anhydrase inhibitory actions*, 84 (2019) 260–268.

54 A.-M. Alaa, A. S. El-Azab, A. H. Ghiaty, P. Gratteri, C. T. Supuran, A. J. B. C. Nocentini, *4-Substituted benzenesulfonamides featuring cyclic imides moieties exhibit potent and isoform-selective carbonic anhydrase II/IX inhibition*, 83 (2019) 198–204.

55 A.-M. Alaa, A. S. El-Azab, M. A. A. El-Enin, A. A. Almehizia, C. T. Supuran and A. J. Nocentini, Synthesis of novel isoindoline-1, 3-dione-based oximes and benzenesulfonamide hydrazones as selective inhibitors of the tumor-associated carbonic anhydrase IX, *Bioorg. Chem.*, 2018, **80**, 706–713.

56 A. Angeli, A.-M. Alaa, A. Nocentini, A. S. El-Azab, P. Gratteri, C. T. J. B. Supuran, M. Chemistry, *Synthesis and carbonic anhydrase inhibition of polycyclic imides incorporating N-benzenesulfonamide moieties*, 25 (2017) 5373–5379.

57 M. A. Mohamed, A.-M. Alaa, H. M. Sakr, A. S. El-Azab, S. Bua, C. T. J. B. Supuran, m. chemistry, *Synthesis and human/bacterial carbonic anhydrase inhibition with a series of sulfonamides incorporating phthalimido moieties*, 25 (2017) 2524–2529.

58 A.-M. Alaa, A. Angeli, A. S. El-Azab, M. A. A. El-Enin, C. T. J. B. Supuran, M. Chemistry, *Synthesis and biological evaluation of cyclic imides incorporating benzenesulfonamide moieties as carbonic anhydrase I, II, IV and IX inhibitor*s, 25 (2017) 1666–1671.

59 A. S. El-Azab, A.-M. Alaa, R. R. Ayyad, M. Ceruso, C. T. J. B. Supuran and M. Chemistry, *Inhibition of carbonic anhydrase isoforms I, II, IVVII and XII with carboxylates and sulfonamides incorporating phthalimide/phthalic anhydride scaffolds*, 24 (2016) 20–25.

60 A.-M. Alaa, A. S. El-Azab, M. Ceruso, C. T. J. B. Supuran and M. C. Letters, *Carbonic anhydrase inhibitory activity of sulfonamides and carboxylic acids incorporating cyclic imide scaffolds*, 24 (2014) 5185–5189.

61 A. A. Abdel-Aziz, A. S. El-Azab, N. A. AlSaif, A. J. Obaidullah, A. M. Al-Obaid and I. A. Al-Suwaidan, Synthesis, potential antitumor activity, cell cycle analysis, and multitarget mechanisms of novel hydrazones incorporating a 4-methylsulfonylbenzene scaffold: a molecular docking study, *J. Enzyme Inhib. Med. Chem.*, 2021, **36**, 1521–1539.

62 G. Xu, M. C. Abad, P. J. Connolly, M. P. Neeper, G. T. Struble, B. A. Springer, S. L. Emanuel, N. Pandey, R. H. Gruninger, M. Adams, S. Moreno-Mazza, A. R. Fuentes-Pesquera and S. A. Middleton, 4-Amino-6-arylamino-pyrimidine-5-carbaldehyde hydrazones as potent ErbB-2/EGFR dual kinase inhibitors, *Bioorg. Med. Chem. Lett.*, 2008, **18**, 4615–4619.

63 S. Şenkardeş, M. Han, N. Kulabaş, M. Abbak, Ö. Çevik, İ. Küçükgüzel and G. Küçükgüzel Ş, Synthesis, molecular docking and evaluation of novel sulfonyl hydrazones as anticancer agents and COX-2 inhibitors, *Mol. Diversity*, 2020, **24**, 673–689.

64 S. Vogel, D. Kaufmann, M. Pojarová, C. Müller, T. Pfaller, S. Kühne, P. J. Bednarski and E. von Angerer, Aroyl hydrazones of 2-phenylindole-3-carbaldehydes as novel antimitotic agents, *Bioorg. Med. Chem.*, 2008, **16**, 6436–6447.

65 R. F. George, Facile synthesis of simple 2-oxindole-based compounds with promising antiproliferative activity, *Future Med. Chem.*, 2018, **10**, 269–282.

66 R. H. Shoemaker, The NCI60 human tumour cell line anticancer drug screen, *Nat. Rev. Cancer*, 2006, **6**, 813–823.

67 M. R. Grever, S. A. Schepartz and B. A. Chabner, The National Cancer Institute: cancer drug discovery and development program, *Semin. Oncol.*, 1992, **19**, 622–638.

68 M. A. El-Sayed, N. I. Abdel-Aziz, A. A. Abdel-Aziz, A. S. El-Azab, Y. A. Asiri and K. E. Eltahir, Design, synthesis, and biological evaluation of substituted hydrazone and pyrazole derivatives as selective COX-2 inhibitors: Molecular docking study, *Bioorg. Med. Chem.*, 2011, **19**, 3416–3424.

69 A. M. Alanazi, A. S. El-Azab, I. A. Al-Suwaidan, K. E. ElTahir, Y. A. Asiri, N. I. Abdel-Aziz and A. A. Abdel-Aziz, Structure-based design of phthalimide derivatives as potential cyclooxygenase-2 (COX-2) inhibitors: anti-inflammatory and analgesic activities, *Eur. J. Med. Chem.*, 2015, **92**, 115–123.

70 J. L. Nakamura, The epidermal growth factor receptor in malignant gliomas: pathogenesis and therapeutic implications, *Expert Opin. Ther. Targets*, 2007, **11**, 463–472.

71 R. M. Hudziak, J. Schlessinger and A. Ullrich, Increased expression of the putative growth factor receptor p185HER2 causes transformation and tumorigenesis of NIH 3T3 cells, *Proc. Natl. Acad. Sci. U. S. A.*, 1987, **84**, 7159–7163.

72 A. Badache and A. Gonçalves, The ErbB2 signaling network as a target for breast cancer therapy, *J. Mammary Gland Biol. Neoplasia*, 2006, **11**, 13–25.

73 U. Asghar, A. K. Witkiewicz, N. C. Turner and E. S. Knudsen, The history and future of targeting cyclin-dependent kinases in cancer therapy, *Nat. Rev. Drug Discovery*, 2015, **14**, 130–146.

74 I. Vermes, C. Haanen, H. Steffens-Nakken and C. Reutelingsperger, A novel assay for apoptosis. Flow cytometric detection of phosphatidylserine expression on early apoptotic cells using fluorescein labelled Annexin V, *J. Immunol. Methods*, 1995, **184**, 39–51.

75 P. K. Parida, B. Mahata, A. Santra, S. Chakraborty, Z. Ghosh, S. Raha, A. K. Misra, K. Biswas and K. Jana, Inhibition of cancer progression by a novel trans-stilbene derivative through disruption of microtubule dynamics, driving G2/M arrest, and p53-dependent apoptosis, *Cell Death Dis.*, 2018, **9**, 448.

76 G. M. Morris, R. Huey, W. Lindstrom, M. F. Sanner, R. K. Belew, D. S. Goodsell, A. J. J. J. O. C. C. Olson, *AutoDock4 and AutoDockTools4: Automated docking with selective receptor flexibility*, 30 (2009) 2785–2791.

77 N. K. K. Ikram, J. D. Durrant, M. Muchtaridi, A. S. Zalaludin, N. Purwitasari, N. Mohamed, A. S. A. Rahim, C. K. Lam, Y. M. Normi, N. A. J. J. o. c. i. Rahman, *Modeling, A virtual screening approach for identifying plants with anti H5N1 neuraminidase activity*, 55 (2015) 308–316.

78 A. Hamdi, W. M. Elhusseiny, D. I. Othman, A. Haikal, A. H. Bakheit, A. S. El-Azab, M. H. Al-Agamy, A.-M. J. E. J. O. M. C. Alaa, *Synthesis, antitumor, and apoptosis-inducing activities of novel 5-arylidenethiazolidine-2, 4-dione derivatives: histone deacetylases inhibitory activity and molecular docking study*, 244 (2022).

79 A. S. El-Azab, Y. S. Mary, C. Y. Panicker, A.-M. Alaa, M. A. El-Sherbeny and C. Van Alsenoy, DFT and experimental (FT-IR and FT-Raman) investigation of vibrational spectroscopy and molecular docking studies of 2-(4-oxo-3-phenethyl-3, 4-dihydroquinazolin-2-ylthio)-N-(3, 4, 5-trimethoxyphenyl) acetamide, *J. Mol. Struct.*, 2016, **1113**, 133–145.

80 A. S. El-Azab, A. M. Alanazi, N. I. Abdel-Aziz, I. A. Al-Suwaidan, M. A. El-Sayed, M. A. El-Sherbeny and A.-M. Alaa, Synthesis, molecular modeling study, preliminary antibacterial, and antitumor evaluation of N-substituted naphthalimides and their structural analogues, *Med. Chem. Res.*, 2013, **22**, 2360–2375.

81 A. A. Abdel-Aziz, A. S. El-Azab, A. M. Alanazi, Y. A. Asiri, I. A. Al-Suwaidan, A. R. Maarouf, R. R. Ayyad and T. Z. Shawer, Synthesis and potential antitumor activity of 7-(4-substituted piperazin-1-yl)-4-oxoquinolines based on ciprofloxacin and norfloxacin scaffolds: in silico studies, *J. Enzyme Inhib. Med. Chem.*, 2016, **31**, 796–809.

82 H. A. Abuelizz, M. Marzouk, A. Bakhiet, M. M. Abdel-Aziz, E. Ezzeldin, H. Rashid and R. J. M. P. Al-Salahi, *In silico study and biological screening of benzoquinazolines as potential antimicrobial agents against methicillin-resistant Staphylococcus aureus, carbapenem-resistant Klebsiella pneumoniae, and fluconazole-resistant Candida albicans*, 160 (2021).